Check for updates

International Journal of Energy Research

WILEY

RESEARCH ARTICLE OPEN ACCESS

Experimental Investigation of the Surface Temperature Effect on Exergy Loss in Photovoltaic Panels With Different Materials and Tilts

Hacer Akhan | Mert Bora Hazar

Department of Mechanical Engineering, Trakya University, Edirne 22030, Türkiye

Correspondence: Hacer Akhan (hacera@trakya.edu.tr)

Received: 19 June 2026 | **Revised:** 13 August 2026 | **Accepted:** 25 August 2026

Keywords: energy–exergy efficiency | exergy loss coefficient | photovoltaic | solar energy

ABSTRACT

This study experimentally investigates the energy and exergy performance of monocrystalline and polycrystalline silicon photovoltaic (PV) panels at different tilts and introduces the concept of the surface temperature-dependent exergy loss coefficient. In the study, the effect of an increase in panel surface temperature on exergy losses was systematically analyzed, and a new performance metric expressing this effect as a dimensionless coefficient was developed. Under the climatic conditions of Edirne, Turkey, surface temperature, electrical power output, and meteorological data for monocrystalline and polycrystalline silicon PV panels were recorded using precise sensors throughout August and September 2025 under identical conditions. The obtained data were evaluated for energy–exergy efficiency and analysis of the surface temperature-dependent exergy loss coefficient. Using multivariate regression analysis, a mathematical model of the exergy loss coefficient as a function of surface temperature was developed, accounting for panel type, surface temperature, PV panel tilt, solar irradiance, ambient temperature, and wind speed. According to analyses based on data obtained from experimental studies, the critical temperature at which the exergy loss coefficient changes for both panels is in the range of 35–45°C (310.15–318.15 K). Within the critical temperature range, the dimensionless exergy loss coefficient for polycrystalline and monocrystalline silicon PV panels ranges from 19 to 23. For monocrystalline silicon PV panels, the exergy loss coefficient is 1–2 units lower than that of polycrystalline PV panels. The fact that the coefficient takes on low values indicates that the increase in panel surface temperature has a limited effect on exergy loss and that the panel is more resistant to temperature increases. The proposed coefficient enhances the comparability of PV systems across different climates and panel types and also provides a new standard for performance evaluation in hot climates.

Highlights

- The exergy loss coefficient dependent on surface temperature is a new characteristic number that measures the sensitivity of exergy loss in photovoltaic (PV) panels to the temperature increase.
- According to analyses performed with data obtained from experimental studies, the critical temperature at which the exergy loss coefficient changes tilt is in the range of 35–45°C.
- In August and September, the highest values in electricity generation from PV panels at a 30° tilt were recorded under the climatic conditions of Edirne.
- The exergy efficiency values of monocrystalline panels are approximately 2%–5% higher than those of polycrystalline panels.

This is an open access article under the terms of the Creative Commons Attribution License, which permits use, distribution and reproduction in any medium, provided the original work is properly cited.

Copyright © 2026 Hacer Akhan and Mert Bora Hazar. *International Journal of Energy Research* published by John Wiley & Sons Ltd.

1 | Introduction

Solar energy is one of the most rapidly developing and widely used technologies among sustainable energy sources. Photovoltaic (PV) panels play a significant role in energy production because they directly convert solar radiation into electrical energy. However, the performance of PV systems varies depending on parameters such as panel type, tilt, environmental conditions, and surface temperature. An increase in panel surface temperature leads to a decrease in efficiency and an increase in thermodynamic irreversibility. For this reason, surface temperature emerges as a critical parameter in the energy and exergy analyses of PV systems.

The effect of surface temperature on the efficiency in PV panels varies depending on the crystal structure of the cell material. Although monocrystalline and polycrystalline silicon cells are produced from the same basic semiconductor material, they differ in terms of the crystal lattice structure and purity. This difference affects their performance response to temperature increases. Since monocrystalline silicon cells consist of a single crystal structure, the movement of electrons encounters fewer obstacles. This ordered structure limits carrier losses associated with temperature increases, thereby keeping efficiency losses at a relatively lower level. In the literature, the typical temperature coefficient for monocrystalline panels is reported to be approximately –0.35%/°C. This value indicates that panel efficiency decreases by approximately 0.35% for every 1°C increase in surface temperature [1, 2]. Polycrystalline silicon cells, on the other hand, consist of a combination of numerous crystalline grains. This structural irregularity hinders electron movement at grain boundaries and increases carrier losses as the temperature rises. Consequently, polycrystalline panels have a higher temperature coefficient, typically around –0.45%/°C. This means that under the same temperature increase conditions, polycrystalline panels experience greater efficiency loss compared to monocrystalline panels [1, 3].

There are numerous studies in the literature on the energy and exergy performance of PV panels at different tilts. These studies have generally focused on determining the optimal tilt, comparing panel types, and calculating the exergy efficiency. However, there is no unique performance metric in the literature that expresses the direct effect of surface temperature on exergy losses using a dimensionless coefficient.

The performance of PV systems varies not only depending on the panel technology used but also on the installation angle, environmental conditions, and thermodynamic parameters. Therefore, to evaluate the system efficiency, it is necessary to use not only energy production metrics but also more comprehensive thermodynamic methods such as exergy analysis. Exergy analysis provides the ability to assess the quality of energy conversion processes by revealing how much "usable energy" a system can produce. Exergy calculations performed using parameters such as panel surface temperature, ambient temperature, and irradiance values reveal the system's thermodynamic suitability. This analysis plays a critical role, particularly in comparisons involving different panel materials (monocrystalline and polycrystalline silicon) and tilts.

There are studies in the literature that experimentally examine the energy and exergy performance of PV panels in terms of both different tilts and different material types. However, research that addresses these two parameters together within the framework of a systematic and simultaneous energy–exergy analysis is quite limited. This indicates that the subject remains a research area with potential for originality. For example, Kumar and Tiwari tested monocrystalline and polycrystalline PV panels at tilts of 15°, 30°, 45°, and 60° and conducted a comparative analysis of both their energy and exergy efficiencies. The study concluded that a 30° tilt offers optimal performance, and it was also observed that polycrystalline panels suffer greater exergy loss at high temperatures [4]. Similarly, Al-Shamani [5] experimentally examined amorphous silicon, CIGS, and crystalline silicon PV modules at different tilts and evaluated the energy and exergy efficiencies for each material type. It was reported that CIGS panels offer high exergy efficiency at a 45° tilt, while amorphous silicon panels demonstrate more stable performance under low irradiance conditions [5]. Fouad et al. [6], on the other hand, tested monocrystalline, polycrystalline, and CdTe panels at different tilts throughout the year in a Mediterranean climate and compared their energy and exergy efficiencies using seasonal tilt optimization. The study demonstrated that steeper tilts increase exergy efficiency during the winter months; it was noted that CdTe panels offer high exergy efficiency under low irradiance, while monocrystalline panels exhibit superior energy performance during the summer months [6]. These examples demonstrate that the tilt is a critical parameter in PV system design not only for light absorption but also for thermodynamic efficiency. However, most existing studies are limited either to a small number of material types or to short-term experimental data. Therefore, an experimental approach based on long-term and simultaneous energy–exergy analysis for various PV materials at different tilts could be considered a novel and contributory study to the literature.

Studies in the literature consistently highlight the complex aspects of angle optimization and its impact on the efficiency of solar energy systems. For example, research conducted by Xie and Lira-Cantu [7] demonstrates that an optimal tilt maximizes PV output by effectively capturing solar radiation throughout the year. The findings of this study also support this claim, revealing that panels tilted at specific angles lead to improvements in energy output and exergy efficiency metrics. Additionally, comparative evaluations highlight the differences between fixed and adjustable tilt systems [7]. The literature, such as Ahmed et al. [8], suggests that adjustable systems can dynamically respond to seasonal changes, thereby enhancing performance under variable conditions. The analysis results in this study yielded a similar finding, showing that tilt adjustments significantly increase energy production during hours of high solar irradiance [8]. When combined with findings from similar studies, strategically adjusting tilts is a critical mechanism not only for maximizing energy but also for reducing entropy-based losses; this topic has been addressed in Bejan's foundational work on exergy [9]. Elbrashy et al. [10] examined the integration of mechatronic systems with renewable energy technologies. The study demonstrates that AI- and IoT-supported mechatronic applications can enhance energy efficiency in solar, wind, geothermal, hydropower, and bioenergy systems by 10%–30%, while

ijer, 2026, 1, Downloaded from https://onlinelibrary.wiley.com/doi/10.1155/er/1293591 by Hacer AKHAN - Trakya Universitesi , Wiley Online Library on [23/09/2026]. See the Terms and Conditions (https://onlinelibrary.wiley.com/terms-and-conditions) on Wiley Online Library for rules of use; OA articles are governed by the applicable Creative Commons License

reducing payback periods by 20%–30% [10]. Elbrashy et al. [11] investigated the design and performance of a hybrid PV/T solar dryer that integrates a steel mesh-enhanced air channel with an independent PV-powered forced airflow. The findings revealed that the system effectively reduced moisture content in mint and apples while achieving a thermal efficiency of 57.3% and an electrical efficiency of 16.2% [11].

As part of this study, the performance of monocrystalline and polycrystalline silicon PV panels at tilts of 0°, 10°, 20°, 30°, and 40° was experimentally investigated under the climatic conditions of Edirne. Meteorological data, panel surface temperature, and electrical output data were measured and recorded using sensors. The obtained data were used in energy and exergy analyses of PV panels. As a result of these analyses, the energy and exergy performance of the PV panels under different tilts was experimentally investigated, and the effect of panel surface temperature on exergy losses was demonstrated using a new performance indicator. In this context, the "surface temperature-dependent exergy loss coefficient" defined for the first time in the literature was developed and tested using experimental data. The study aims to provide a comparable analysis across different climatic conditions and panel types by expressing the critical role of surface temperature in evaluating the PV system performance through a dimensionless coefficient. The scope of the research is defined as follows:

- Experimental measurements were conducted on monocrystalline and polycrystalline silicon PV panels installed at different tilts under Edirne's climatic conditions.
- During the measurements, panel surface temperature, ambient temperature, solar irradiance, and electrical outputs were measured and recorded at 1 min intervals.
- Energy efficiency and exergy efficiency were calculated to obtain classical performance indicators.
- Using the newly defined exergy loss coefficient, the effect of surface temperature on exergy losses was expressed in a dimensionless form. The exergy loss coefficient dependent on surface temperature was modeled using multiple regression analysis, considering panel type, surface temperature, PV panel tilt, solar irradiance, ambient temperature, and wind speed. The results were evaluated comparatively under different tilts and climatic conditions. By adding a third dimension alongside energy efficiency and exergy efficiency, it provides a more comprehensive analysis. This coefficient, which serves as a normalized performance indicator, normalizes the exergy loss of the PV panel due to surface temperature relative to the incoming solar exergy and ambient temperature, thereby enabling the comparison of different panels or different climatic conditions. It demonstrates how quickly the panel loses its exergy efficiency in response to a temperature increase with the aim of measuring marginal sensitivity. In other words, it quantitatively expresses the relative response to temperature. By identifying critical temperature ranges, it reveals in which temperature ranges the panel's performance degradation is more pronounced. This is important for panel selection and cooling strategies in field applications. In this context, the study aims to provide a unique contribution to the performance analysis of PV systems and to more clearly highlight the effect of surface temperature in hot climates.

2 | Materials and Methods

2.1 | Characteristic of the Installation Site

Edirne is located between 41° and 40° north latitude and 26° and 34° east longitude [12]. With a total area of 6098 km^2, Edirne lies approximately 41 m above sea level. Due to its location, the city is a transitional region influenced by both the Mediterranean climate and the continental climate typical of Central Europe. During summer, temperatures do not drop below 30°C; the highest solar radiation values are recorded in June, while the longest duration of sunshine is observed in July. The variation in solar radiation for August and September at the installation site is shown in Figure 1, the variation in ambient temperature in Figure 2, and the average wind speed in Figure 3. Figures 1–3 were generated using the data measured by the meteorological station at the system installation site. The study is limited to

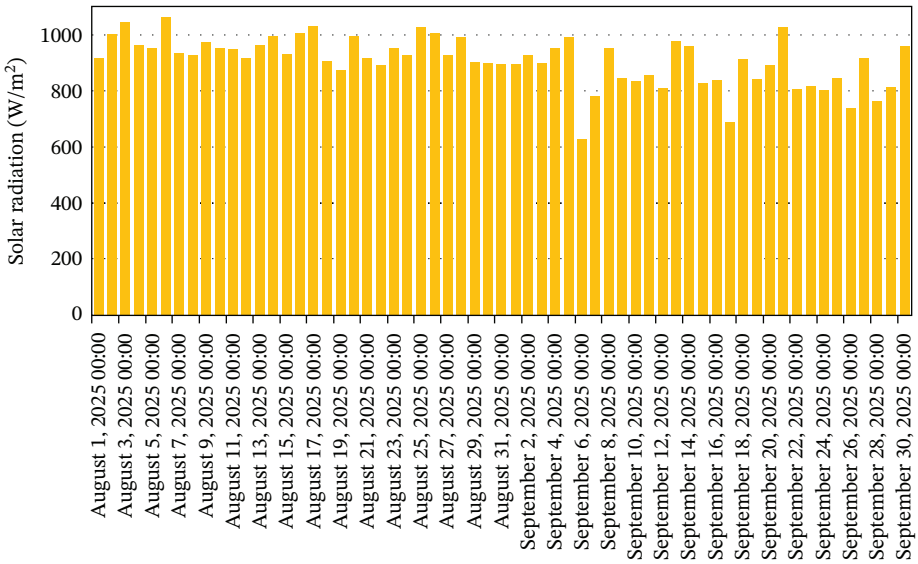


FIGURE 1 | Solar radiation values for August and September at the installation site.

ijer, 2026, 1, Downloaded from https://onlinelibrary.wiley.com/doi/10.1155/er/1293591 by Hacer AKHAN - Trakya Universitesi , Wiley Online Library on [23/09/2026]. See the Terms and Conditions (https://onlinelibrary.wiley.com/terms-and-conditions) on Wiley Online Library for rules of use; OA articles are governed by the applicable Creative Commons License

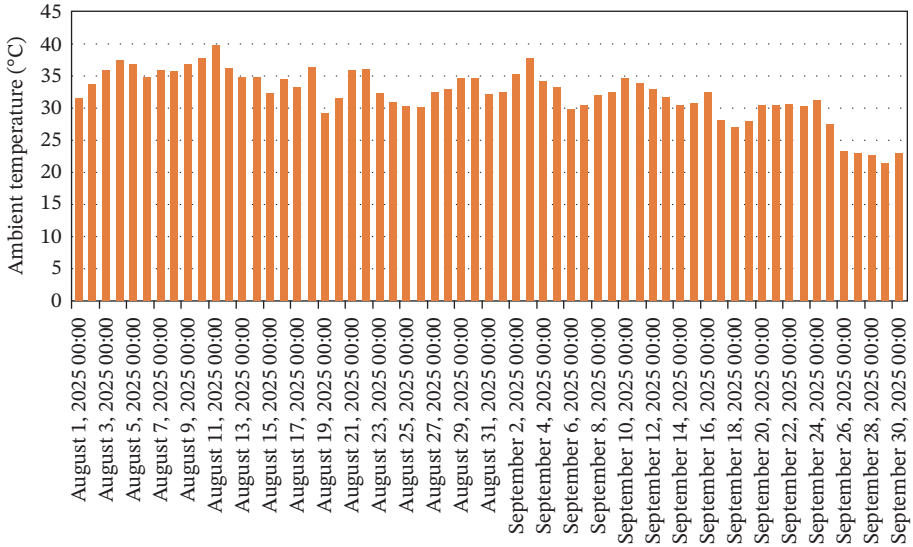


FIGURE 2 | Ambient temperature values for August and September at the installation site.

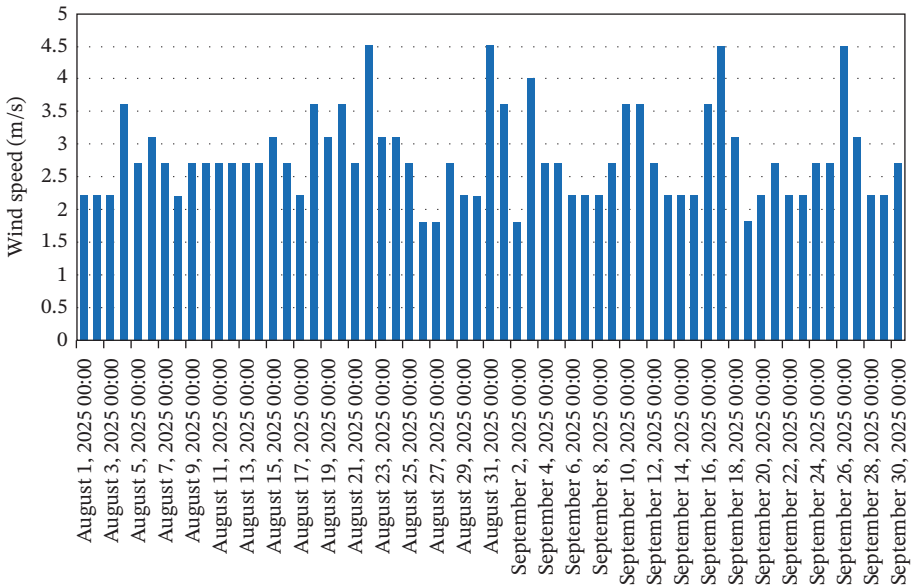


FIGURE 3 | Wind speed values for August and September at the installation site.

measurements taken in Edirne during August and September. However, this period represents the critical production months for PV systems in Edirne; while August provides maximum production with high irradiance values, September increases efficiency with lower irradiance but more favorable temperature conditions. For this reason, the findings serve as a meaningful reference point for optimizing regional PV performance.

2.2 | The Experimental Setup

In the present study, the PV system was installed at the Energy Field of the Faculty of Engineering, Trakya University, positioned at 41° 38′ 0″ N and 26° 37′ 26″ E. In the experimental studies conducted, an off-grid PV panel system made of monocrystalline and polycrystalline silicon materials was used. Figure 4 shows a schematic diagram of the PV system and Figure 5 shows a photograph of the PV panels. One polycrystalline silicon PV panel and one monocrystalline silicon PV panel were operated simultaneously under identical environmental conditions at different tilts. Thus, the materials were tested concurrently, and the tilt angles were varied simultaneously during the measurements. The panels were repositioned at different times to new tilts, and measurements were repeated under varying atmospheric conditions. The PV panels were mounted on a mechanical structure that could be adjusted to different tilts and tested at tilts of 0°, 10°, 20°, 30°, and 40°. The system was positioned with an azimuth angle of 0°. The surfaces of the PV panels were cleaned regularly, and the panels were mounted in such a way that there would be no shading effect during operation.

Electricity is generated as direct current (DC) in the PV panel. It is then converted to alternating current (AC) in the inverter. Table 1 lists the nominal technical specifications of the PV panel determined under standard test conditions of 1000 kW and 25°C. PV panels with the same cell configuration and very similar dimensions were used in both systems. Figure 6a shows

ijer, 2026, 1, Downloaded from https://onlinelibrary.wiley.com/doi/10.1155/er/1293591 by Hacer AKHAN - Trakya Universitesi , Wiley Online Library on [23/09/2026]. See the Terms and Conditions (https://onlinelibrary.wiley.com/terms-and-conditions) on Wiley Online Library for rules of use; OA articles are governed by the applicable Creative Commons License

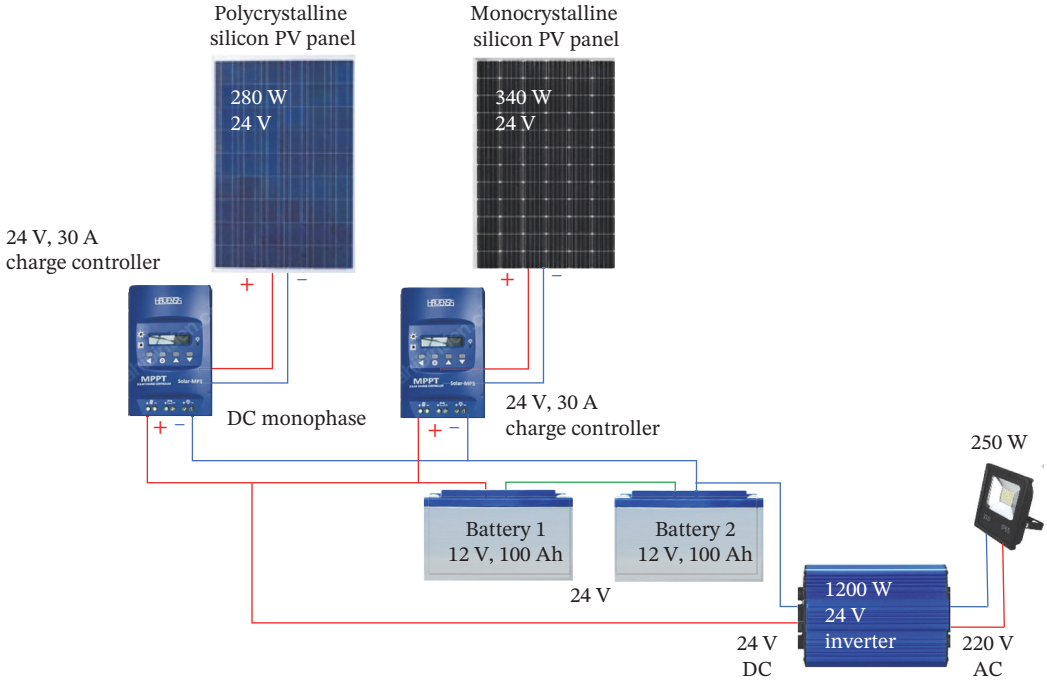


FIGURE 4 | Schematic diagram of a PV system.



FIGURE 5 | Polycrystalline and monocrystalline silicon PV panels.

polycrystalline and monocrystalline PV panels at a 0° tilt, Figure 6b at 10°, Figure 6c at 20°, Figure 6d at 30°, and Figure 6e at 40°. The PV panels were operated under the same environmental conditions and tilts during the measurements. Table 2 shows the technical specifications of the MPPT charge controller.

2.3 | Data Collection System

The solar radiation, outdoor temperature, wind speed and direction, and outdoor humidity at the site where the Trakya University weather station was installed were measured continuously 24 h a day, 7 days a week, under all weather conditions. Remote access to the weather station data allows for data monitoring, downloading, and saving via a computer and mobile phone. Current, voltage, and power output data from the PV panels were measured at 1 min intervals via the MPPT charge controller and recorded using the remote access module. Figure 7a shows the weather station and pyranometer. Since tilt comparisons require not only irradiance measured at a horizontal meteorological station but also plane-of-array irradiance, solar irradiance was measured both at the meteorological station and on a surface placed at the same tilt angle as the PV panels using an external pyranometer to record the irradiance incident on the tilted plane. In our study, the calculations were performed using the irradiance measured directly on the tilted PV panel surface, rather

TABLE 1 | Technical specifications of PV panels.

Property	Value	
Cell type	Polycrystalline	Monocrystalline
Cell arrangement	60 (60 × 1)	60 (60 × 1)
Dimensions	1640 × 990 × 35 mm	1660 × 1001 × 35 mm
Weight	19 kg	19 kg
Front laminate	3.2 mm tempered glass	3.2 mm tempered glass
Frame material	Aluminum alloy	Aluminum alloy
J-Box	IP67	IP67
Cable	4 mm^2 (IEC)/ 12AWG (UL)	4 mm^2 (IEC)/ 12AWG (UL)
Nominal Max. power	280 W	340 W
Optimum operating voltage	31.2 V	34.98 V
Optimum operating current	8.97 A	9.72
Open-circuit voltage (V_{oc})	37.8 V	42.56 V
Short-circuit current (I_{sc})	9.50 A	9.99 A
Module efficiency	19%	23%
Operating temperature	−40 to +85°C	−40 to +85°C

ijer, 2026, 1, Downloaded from https://onlinelibrary.wiley.com/doi/10.1155/er/1293591 by Hacer AKHAN - Trakya Universitesi , Wiley Online Library on [23/09/2026]. See the Terms and Conditions (https://onlinelibrary.wiley.com/terms-and-conditions) on Wiley Online Library for rules of use; OA articles are governed by the applicable Creative Commons License



FIGURE 6 | Polycrystalline and monocrystalline PV panels for different tilts. (a) 0°, (b) 10°, (c) 20°, (d) 30°, and (e) 40°.

TABLE 2 | Technical specifications of MPPT charge controller.

Property	Value
Model	Solar-30 A MPPT
Nominal system voltage	12/24 V Automatic Operation
Nominal charge current	30 A
Nominal load current	20 A
Battery input voltage	9–32 V DC
MPP voltage range	Battery voltage + 2–90 V
Self-consumption current loss	<30 mA @12 V; <20 mA @24 V (25°C)
Temperature compensation	−20 mV/PC/12 V (25°C)
Accuracy	±1% of full-scale voltage reading
Overcurrent protection (15 s)	Load current × 1.25
Short-circuit protection	Load current × 2
Operating temperature	−30°C to +60°C
Communication port	RS-232/RS-485 (RJ11 Socket), MODBUS-RTU

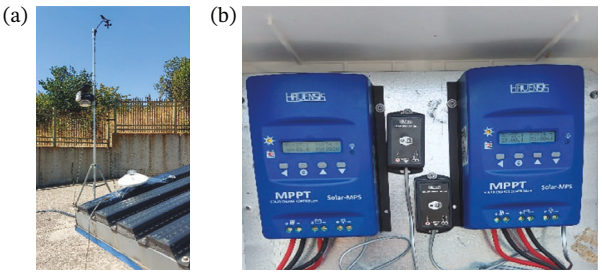


FIGURE 7 | (a) Davis Vantage Pro2 wireless weather station and pyranometer and (b) MPPT charge controllers and remote access modules.

than the horizontal meteorological station data. This approach was adopted to ensure that the performance analysis accurately reflects the actual operating conditions of the panels. Figure 7b shows the MPPT charge controllers and remote access modules the MPPT charge controllers and remote access modules. To determine the power output of each panel separately, a separate MPPT charge controller was used for each PV panel. The surface temperatures of the PV panels were measured using PT100 temperature sensors mounted on the panels and stored via a data logger at 1 min intervals.

ijer, 2026, 1, Downloaded from https://onlinelibrary.wiley.com/doi/10.1155/er/1293591 by Hacer AKHAN - Trakya Universitesi , Wiley Online Library on [23/09/2026]. See the Terms and Conditions (https://onlinelibrary.wiley.com/terms-and-conditions) on Wiley Online Library for rules of use; OA articles are governed by the applicable Creative Commons License

TABLE 3 | Technical specifications of Davis Vantage Pro2 wireless weather station.

Parameter	Sensor type	Range	Accuracy
Temperature	PN junction silicon diode	−40 to +65°C	±0.5°C
Solar radiation	Silicon photodiode sensor	0–1800 W/m^2	±5%
UV index	Photodiode UV sensor	0–16	±5%
Humidity	Film capacitor element	0%–100% RH	±3% RH
Wind speed	Magnetic wind cups	1–89 m/s (2–200 mph)	±5% of reading
Wind direction	Magnetic encoder wind vane	0°–360°	±3°
Rainfall	Tipping spoon rain collector	0–9999 mm	±4%
Barometric pressure	Piezo-resistive pressure sensor	540–1100 hPa	±1.0 hPa

TABLE 4 | Technical specifications of pyranometer.

Property	Value
Category	CM6B
ISO classification	First class
Response time 95% (s)	18
Thermal radiation (200 W/m^2)	<15 W/m^2
Temperature change (5K/h)	<±4 W/m^2
Nonstability (% change/year)	±1 max
Directional error (at 1000 W/m^2)	<±20 W/m^2
Tilt response (±80° at 1000 W/m^2)	<±1%
Level accuracy (°)	0.5
Sensitivity (μV/[W/m^2])	9–15
Spectral range (50% points, nm)	305–2800
Expected signal output (atmospheric)	0–25 mV

TABLE 5 | Technical specifications of datalogger.

Property	Value
Model	Graphtech GL260
Input types	Voltage (20 mV–100 V), temperature (K, J, E, T, R, S, B, N, C), current (4–20 mA), humidity (0%–100% RH)
Sampling rate	Minimum 10 ms (for 1 channel); up to 10 channels measured within 100 ms
Data storage	8 GB internal flash memory; SDHC card support (up to 32 GB)
Power options	AC adapter (100–240 V), DC input (8.5–24 V), optional battery pack (7.2 V, 2875 mAh)
Display and user interface	4.3-inch TFT color LCD (480 × 272 pixels); user-friendly menu structure
Effective resolution	1/40,000 of ± measurement range
Voltage accuracy	Typically within ±0.1% of full scale
Temperature accuracy	±1 to ±2°C
Humidity accuracy	±2%–3% RH

Table 3 presents the technical specifications of the Davis Vantage Pro2 wireless weather station, Table 4 presents the pyranometer, Table 5 presents the data logger, Table 6 presents the PT100 sensors, and Table 7 presents the remote access module.

TABLE 6 | Technical specifications of PT100.

Property	Value
Sensor type	Platinum resistance temperature detector (RTD)
Nominal resistance	100 Ω at 0°C
Temperature range	0–100°C
Accuracy classes	Class A: ±(0.15 + 0.002)
Applications	Energy systems
Connection types	2 wire
Calibration standard	IEC 60751 (International standard for RTDs)

2.4 | Analysis Method

2.4.1 | PV System Energy Analysis Method

The output power of PV panels is significantly affected by weather conditions, solar irradiance, and panel temperature. The power generation of a PV panel varies from the value obtained under standard test conditions depending on the solar irradiance on the PV panel and the ambient temperature, and the energy input varies depending on the solar irradiance on the PV panel. The output power P_{PV} (Watts) of a PV panel with the operating voltage V_{PV} (V) and current I_{PV} (A) is expressed by Equation (1). N_{PV} represents the number of PV panels.

$$P_{PV} = V_{PV} . I_{PV} . N_{PV}. \quad (1)$$

$\dot{E}_{in}$ is the power entering the PV panel (W) and is calculated using Equation (2) [13].

$$\dot{P}_{in} = A \times G, \quad (2)$$

ijer, 2026, 1, Downloaded from https://onlinelibrary.wiley.com/doi/10.1155/er/1293591 by Hacer AKHAN - Trakya Universitesi , Wiley Online Library on [23/09/2026]. See the Terms and Conditions (https://onlinelibrary.wiley.com/terms-and-conditions) on Wiley Online Library for rules of use; OA articles are governed by the applicable Creative Commons License

TABLE 7 | Technical specifications of the remote access module.

Property	Value
Communication protocols	RS232/RS485 (via MSMPORT), Modbus-RTU
Wireless connectivity	Wi-Fi module support (IEEE 802.11 b/g/n)
Installation	RJ45/RS232 cable connection; magnetic mounting option
Power supply	Powered directly from MPPT controller
Operating temperature	−10 to +55°C
Protection	Compact design, typically <100 mm × 60 mm × 25 mm
Current measurement accuracy	±1% of measured current
Voltage measurement accuracy	±1% of full-scale reading

where A is defined as the surface area of the PV panel (m^2), and G as the solar irradiance value (W/m^2). $\dot{E}_{out}$, the net power output of the PV panel (W), is calculated using Equation (3) [14].

$$\dot{P}_{out} = P_{max}, \tag{3}$$

$$P_{max} = I_{SC} \times V_{OC} \times FF, \tag{4}$$

where FF is the fill factor. In other words, the fill factor is the ratio of the maximum output power to the product of the open-circuit voltage (V_{OC}) and the short-circuit current (I_{SC}). The fill factor is typically used to indicate the quality of a PV module's power generation.

$$FF = \frac{I_{max} \times V_{max}}{I_{SC} \times V_{OC}}. \tag{5}$$

η_{PV} is calculated using Equation (6) as the ratio of the PV panel's energy output to its energy input [14].

$$\eta_{PV} = \frac{\dot{P}_{out}}{P_{in}}. \tag{6}$$

2.4.2 | Exergy Analysis Method for PV Systems

Exergy analysis is important for determining the energy quality and the losses incurred in a system due to irreversibility. Exergy is the ability to perform work. It can be defined as the maximum theoretical useful work that can be obtained from a system from its initial state until it reaches the dead state. Exergy analysis can be performed on all systems that convert energy. This is because exergy is a measure of both quantity and quality. In PV systems, the electrical energy produced by the PV panel represents the system's exergy output. Heat is also generated during the electricity production. This heat results in exergy losses due to irreversibility.

Maximum work can only be obtained in a reversible process. This process can be carried out by utilizing an infinitesimally small temperature difference between the heat sink and the heat source. All real processes in nature are irreversible because they occur with a finite temperature difference. Therefore, the work obtained in these processes has values lower than the maximum that is possible. When evaluating the work obtained, it must be compared to the maximum value in a specific process, namely, exergy. The process is carried out using the environment as a free source of heat and matter. From this, it follows that maximum work is obtained only when matter operates in concert with the environment [15]. In exergy calculations, the thermodynamic equilibrium state, involving common environmental components (such as atmospheric air), is used as a reference [16].

The output exergy rate at the PV panel is expressed by Equation (7). $\dot{E}x_{in}$ (W) is defined as the exergy rate entering the system, $\dot{E}x_{out}$ (W) as the exergy rate leaving the system, and $\dot{E}x_{loss}$ (W) as the exergy rate destroyed. For a PV system, the output exergy rate $\dot{E}x_{out}$ (W) is equal to the difference between the electrical exergy rate $\dot{E}x_e$ (W) and the thermal exergy rate $\dot{E}x_{ther}$ (W). In this case, the exergy balance can be defined by Equation (8) [17].

$$\dot{E}x_{out} = \dot{E}x_{(PV)out} = \dot{E}x_e - \dot{E}x_{ther}, \tag{7}$$

$$\dot{E}x_{in} = \dot{E}x_e - \dot{E}x_{ther} + \dot{E}x_{loss}. \tag{8}$$

The inlet exergy rate of the PV panel $\dot{E}x_{in}$ is equal to the exergy rate of solar radiation $\dot{E}x_{sun}$ (W). $\dot{E}x_{sun}$ is calculated using Equation (9) [18].

$$\dot{E}x_{in} = \dot{E}x_{sun} = A \times G \times \left[1 + \frac{1}{3} \times \left(\frac{T_0}{T_{sun}}\right)^4 - \frac{4}{3} \times \left(\frac{T_0}{T_{sun}}\right)\right]. \tag{9}$$

T_0 (K) is defined as the ambient temperature, and T_{sun} (K) as the solar temperature. The solar temperature is taken as 5770 K in the calculations [18].

The electrical exergy rate generated by the PV panel is determined by the equation given in Equation (10) [18].

$$\dot{E}x_e = V_{OC} \times I_{SC} \times FF. \tag{10}$$

Exergy destruction (loss) is expressed by Equation (11).

$$\dot{E}x_{loss} = T_0 \times \frac{\Delta S_{total}}{\Delta t}. \tag{11}$$

Δt (s) is defined as the change in time, and ΔS_{total} (kJ/K) is defined as the change in total entropy (production).

PV cell temperature has a significant impact on energy and exergy efficiencies. Normal operating cell temperature (NOCT) is a standard metric that defines the temperature reached by solar cells under typical environmental conditions outside the laboratory. Module temperature T_m can be determined using

ijer, 2026, 1, Downloaded from https://onlinelibrary.wiley.com/doi/10.1155/er/1293591 by Hacer AKHAN - Trakya Universitesi , Wiley Online Library on [23/09/2026]. See the Terms and Conditions (https://onlinelibrary.wiley.com/terms-and-conditions) on Wiley Online Library for rules of use; OA articles are governed by the applicable Creative Commons License

Equation (12) with the nominal operating temperature and irradiance value [19]. Under nominal operating conditions, solar irradiance, wind speed, operating temperature, and air mass values are specified. Under nominal operating conditions, the irradiance is assumed to be 1000 W/m^2, the wind speed 1 m/s, the operating temperature 20°C, and the air mass index 1.5 [20]. In the calculations, the value of 45°C specified by the panel manufacturer in its technical specifications was used for the NOCT.

$$T_m = T_0 + (\mathrm{NOCT} - 20)\frac{G}{800}. \tag{12}$$

A PV panel converts absorbed solar radiation into electricity and heat. The electricity generated (converted) by the PV panel is usable energy and can be considered the system's exergy [21]. However, the heat generated is generally not usable and is transferred to the environment. A portion of the heat transferred to the environment can be expressed as an exergy loss for the system [22]. As seen in Equation (13), the exergy efficiency η_{Ex} for a PV panel can be defined as the ratio of the exergy obtained from the PV panel to the exergy possessed by solar radiation [18].

$$\eta_{\mathrm{Ex}} = \frac{\dot{\mathrm{Ex}}_e}{\dot{\mathrm{Ex}}_{\mathrm{in}}}. \tag{13}$$

2.4.3 | Exergy Loss Coefficient as a Function of Surface Temperature

The exergy loss coefficient depending on surface temperature is a new characteristic number that measures the sensitivity of the exergy loss of PV panels to temperature increase and characterizes the response of the PV panel to the surface temperature. Exergy represents a system's potential to perform useful work. As the surface temperature of a PV panel increases, thermodynamic irreversibility increase, which leads to exergy loss. In the coefficient equation, it is not sufficient to present exergy loss alone; it must be normalized with respect to the exergy entering the system. This allows for comparisons under different irradiation conditions. Additionally, the temperature difference is a critical parameter in the exergy analysis. As the temperature difference between the panel surface and the surroundings increases, irreversibility increase. In Equation (22), the coefficient represents "the effect of each 1 K increases on exergy."

As seen in Equation (14), if the temperature difference $(T_S - T_0)$ is used directly in the exergy loss coefficient equation, the unit of the coefficient is 1/K. In this case, the coefficient represents the "exergy loss per unit temperature difference."

$$\theta_{T_S} = \frac{E_{\mathrm{loss}}}{E_{\mathrm{in}} \times (T_S - T_0)}. \tag{14}$$

In Equation (15), the "exergy loss coefficient dependent on surface temperature" expresses the effect of an increase in surface temperature on exergy losses in PV panels as a dimensionless measure. The coefficient consists of two main components: the ratio of exergy loss to input exergy and the normalization of the temperature difference. The first component indicates the extent to which the exergy loss occurring in the panel is significant relative to the exergy entering the system. The second component is obtained by normalizing the difference between the panel surface temperature and the ambient temperature relative to the ambient temperature. This approach normalizes the temperature difference into a ratio, thereby providing a dimensionless performance indicator that is comparable across different climatic conditions. Unlike classical energy and exergy efficiencies, the coefficient directly quantifies the effect of surface temperature on exergy losses using a dimensionless number.

To define the coefficient as a comparable critical value, the temperature difference is normalized. In this case, as shown in Equation (15), all terms become ratios, and the dimensionless exergy loss coefficient $\theta^*_{T_S}$, which depends on the surface temperature, expresses the exergy loss caused by a unit increase in surface temperature relative to the input exergy in dimensionless form. The dimensional coefficient (1/K) directly quantifies the exergy loss of the PV panel relative to the temperature increase. The dimensionless coefficient is more suitable for comparing different panels, climates, and conditions.

$$\theta^*_{T_S} = \frac{E_{\mathrm{loss}}}{E_{\mathrm{in}}} \times \frac{T_0}{(T_S - T_0)}. \tag{15}$$

E_{loss} is defined as the lost exergy, E_G as the exergy from the sun (the usable portion of solar radiation), T_S as the PV panel surface temperature, and T_0 as the ambient (reference) temperature. $\frac{E_{\mathrm{lost}}}{E_{\mathrm{in}}}$ indicates the proportion of usable energy the panel loses out of the total energy it receives from the sun. As this ratio increases, the losses increase. In the numerator $(\frac{T_0}{(T_S - T_0)})$, as the surface temperature increases, the denominator $(T_S - T_0)$ grows, and the coefficient decreases. In other words, the coefficient decreases at high surface temperatures. At low temperatures $(T_S \approx T_0)$, with a small temperature difference, the coefficient is large. In other words, the panel is highly sensitive to the temperature. Even small temperature $(T_S \approx T_0)$ increases raise the coefficient. At high temperatures $(T_S \gg T_0)$, with a large temperature difference, the coefficient is small. In other words, the panel's marginal sensitivity decreases; even if the temperature continues to rise, the coefficient gradually decreases.

Equation (15) shows the exergy loss normalized with respect to the PV panel's surface temperature. The decrease in the coefficient indicates that the panel's marginal sensitivity weakens at high temperatures. In other words, the panel still loses exergy, but its relative response to rising temperatures decreases. This situation demonstrates that the PV panel is thermodynamically linear and that as the temperature increases, the losses enter a more "saturated" regime. Its response to temperature increases and becomes progressively more linear.

The equation shows us the following: as the PV panel's surface temperature increases, the exergy loss grows, but the dimensionless coefficient decreases. This decrease does not mean the panel is more durable; it merely indicates that the relative sensitivity to temperature has decreased, the derivative value $\partial\theta^*_{T_S}/\partial T_S$ has decreased, meaning the tilt of the panel's response curve has decreased. This is because the coefficient indicates the panel's

ijer, 2026, 1, Downloaded from https://onlinelibrary.wiley.com/doi/10.1155/er/1293591 by Hacer AKHAN - Trakya Universitesi , Wiley Online Library on [23/09/2026]. See the Terms and Conditions (https://onlinelibrary.wiley.com/terms-and-conditions) on Wiley Online Library for rules of use; OA articles are governed by the applicable Creative Commons License

normalized marginal sensitivity to temperature increases but not its absolute performance.

The exergy loss coefficient dependent on surface temperature can be used to compare PV panel performance from a thermodynamic perspective, to compare the temperature resistance of monocrystalline and polycrystalline panels, to predict panel performance in different regions (e.g., hot climates), and to evaluate the effectiveness of active/passive cooling methods in PV panels. The purpose of use is to measure sensitivity (to demonstrate how quickly the panel loses exergy efficiency in response to temperature increases), to make comparisons (to compare different panel types and technologies using the same criteria), to determine the critical temperature (to identify the threshold point at which exergy efficiency begins to deteriorate rapidly), and to optimize performance (to minimize the temperature effect on the panel under design and operating conditions).

The exergy loss coefficient depending on surface temperature is not merely a mathematical normalization, but rather a new characteristic number that quantifies the sensitivity of exergy loss to incremental changes in PV panel surface temperature. The coefficient expresses the effect of each 1 K increase in surface temperature on the exergy loss of the PV panel. In this way, it characterizes the thermodynamic response of the panel to temperature variations, which is not captured by conventional exergy efficiency indicators. Exergy represents the potential of a system to perform useful work. As the surface temperature rises, irreversibility increases, leading to exergy loss. By normalizing the loss with respect to the exergy input, the coefficient allows for meaningful comparisons under different irradiation conditions. This normalization is essential to distinguish between absolute losses and the relative sensitivity of the system. Unlike classical exergy efficiency, which provides a static measure of performance, the coefficient introduces a dynamic perspective by quantifying the temperature sensitivity. This enables the comparative evaluation of different PV technologies in terms of their thermal robustness, identification of critical temperature ranges where performance degradation accelerates, and guidance for cooling strategies and design improvements in PV systems.

2.4.4 | Multiple Regression Analysis

In this study, the mathematical modeling of the dimensionless exergy loss coefficient depending on surface temperature under real environmental conditions in the field was carried out for two different PV panels (monocrystalline and polycrystalline). For this purpose, multivariable regression analysis was applied using multiple environmental and electrical variables. The exergy loss coefficient depending on surface temperature is modeled based on panel type, surface temperature, PV panel tilt, solar irradiance, ambient temperature, and wind speed. This system aims to generate data that will contribute to the optimization of small-scale PV systems for sustainable energy production, especially in rural and isolated areas. At the same time, it enables the statistical understanding of multiple parameters affecting panel performance from the perspective of scientific modeling.

Missing data were checked during the data preprocessing stage for multivariate regression analysis. All variables were normalized to make them comparable. Dummy coding was applied for the panel type. During the construction of the regression model, separate regression models were defined for the exergy loss coefficient depending on the surface temperature. The model was created using Excel and Python. Linear and interactive models were tested separately. Model validation and performance were measured using metrics such as R^2 (coefficient of determination), root mean square error (RMSE), and mean absolute error (MAE) to assess model performance. The statistical significance of the models was verified using ANOVA and the F-test. During the parameter analysis stage, the regression coefficients were examined to interpret the effect of each variable on energy and exergy efficiency.

3 | Result and Discussion

3.1 | Power Variation of PV Panels at Different Tilt

As solar irradiance on a PV panel increases, the photon density per unit area rises, which leads to the formation of more electron–hole pairs at the semiconductor junction, thereby increasing the output current. This, in turn, boosts the system's electricity production. Electricity production in PV panels is directly related to the irradiance value perpendicular to the panel surface. Kosin's law states that the irradiance intensity on the panel surface varies with the cosine of the angle of incidence of sunlight. Mathematically, the energy obtained per unit area of the panel depends on the cosine of the angle between the normal of sunlight and the normal of the panel. In this context, the optimal tilt is the angle that minimizes the angle between the sun's path in the sky (zenith angle) and the panel's normal as much as possible.

The power output of PV panels is directly related to the efficiency of the solar radiation that hits the surface and the panel's operating temperature. The panel's tilt affects both parameters simultaneously, causing significant changes in the power output. At the optimal tilt, where the panel surface is positioned more perpendicular to sunlight, the amount of absorbed radiation reaches its maximum level. In this case, the power output reaches its highest level.

Figure 8a at a 0° tilt, Figure 8b at a 10° tilt, Figure 8c at a 20° tilt, Figure 8d at a 30° tilt, and Figure 8e at a 40° tilt show the variation of electrical energy produced by PV panels over time. As seen in Figure 8, the highest power generation was achieved when the PV panel tilt was 30°. Under the same conditions, the power output of the monocrystalline silicon PV panel is higher than that of the polycrystalline silicon PV panel.

Table 8 shows the average daily electricity generation for polycrystalline and monocrystalline silicon PV panels at different tilts. As shown in Table 8, the highest average daily electricity generation was achieved when the PV panel tilt was 30°. Under the same conditions, the energy production of monocrystalline silicon PV panels is higher than that of polycrystalline silicon PV panels.

ijer, 2026, 1, Downloaded from https://onlinelibrary.wiley.com/doi/10.1155/er/1293591 by Hacer AKHAN - Trakya Universitesi , Wiley Online Library on [23/09/2026]. See the Terms and Conditions (https://onlinelibrary.wiley.com/terms-and-conditions) on Wiley Online Library for rules of use; OA articles are governed by the applicable Creative Commons License

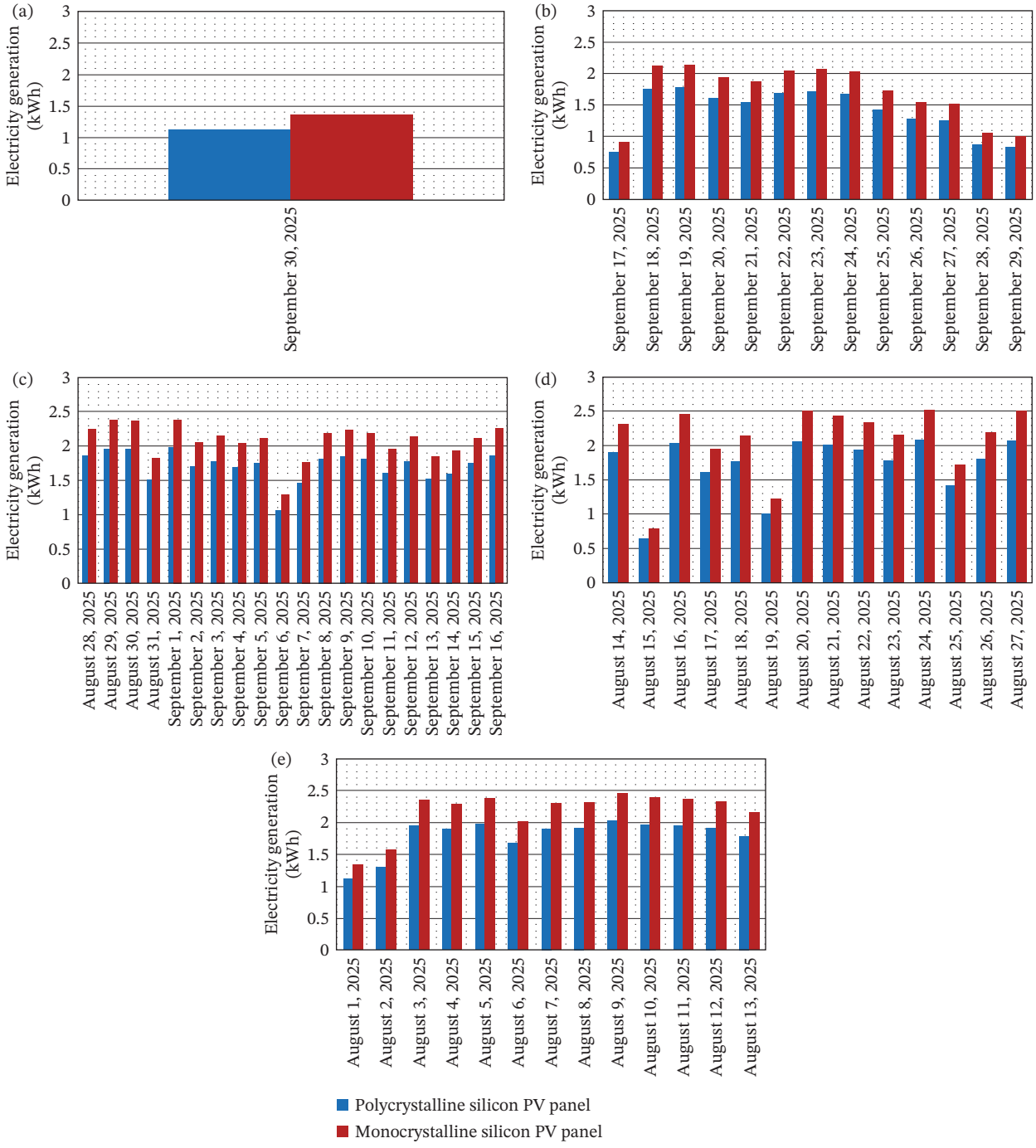


FIGURE 8 | Variation in the electrical energy generated by polycrystalline and monocrystalline silicon PV panels with different tilts over time. (a) 0°, (b) 10°, (c) 20°, (d) 30°, and (e) 40°.

TABLE 8 | Daily average electrical energy production values for polycrystalline and monocrystalline silicon PV panels at different tilts.

	Average daily electricity generation (kWh)	
Panel tilt	**Polycrystalline silicon PV panel**	**Monocrystalline silicon PV panel**
0°	1.116	1.351
10°	1.444	1.748
20°	1.531	1.854
30°	1.787	2.163
40°	1.659	2.002

ijer, 2026, 1, Downloaded from https://onlinelibrary.wiley.com/doi/10.1155/er/1293591 by Hacer AKHAN - Trakya Universitesi , Wiley Online Library on [23/09/2026]. See the Terms and Conditions (https://onlinelibrary.wiley.com/terms-and-conditions) on Wiley Online Library for rules of use; OA articles are governed by the applicable Creative Commons License

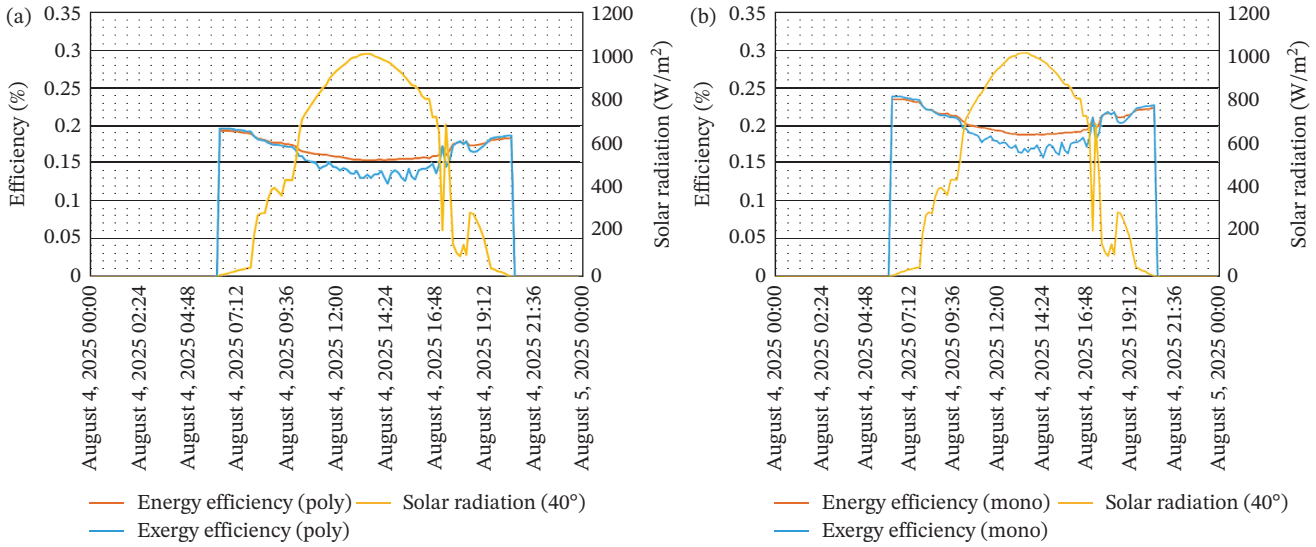


FIGURE 9 | Variation in exergy and energy efficiencies of polycrystalline and monocrystalline silicon PV panels at a 40° tilt. (a) 40° and (b) 40°.

3.2 | Energy and Exergy Efficiency of PV Panels for Different Tilt

The thermodynamic performance analysis of PV systems is conducted using energy analysis, which is based on the principle of energy conservation, and exergy analysis, which measures the potential and quality of energy to perform work. Figure 9a shows the energy and exergy efficiencies of a polycrystalline PV panel at a 40° tilt, while Figure 9b illustrates the variation in the exergy and energy efficiencies of a monocrystalline PV panel.

The fact that exergy efficiency is higher than energy efficiency under conditions of low solar irradiance (in the morning and evening), whereas exergy efficiency is lower than energy efficiency under conditions of high solar irradiance (at midday), is primarily explained by the production of entropy within the system and changes in the temperature gradient between the panel temperature and the ambient temperature. During the morning hours when irradiance is low, the temperature increase on the surface of the PV panel remains limited, and the panel temperature remains close to the reference dead-point (ambient) temperature. When evaluated in the context of the second law of thermodynamics, the panel temperature being close to the ambient temperature ensures that exergy destruction resulting from heat transfer within the system is kept at a minimum. While a portion of the high-quality radiation from the sun (originating from a high-temperature source) is converted into electricity, the panel's lack of heating preserves the ability of the available energy to be converted into work. This situation causes the exergy efficiency to be numerically higher than the energy efficiency at low irradiance levels.

As solar irradiance increases toward midday, the photon density falling on the PV panels rises, and a large portion of this energy, which cannot be converted into electricity, is converted into thermal energy, rapidly raising the panel temperature. The deviation of the panel temperature from the ambient temperature (reference temperature) maximizes irreversibility and entropy production within the system. Exergy analysis assumes that this waste heat at high temperatures is a form of energy and reduces the system's potential to perform work.

As solar irradiance increases, PV exergy and energy efficiency decrease while electrical energy production increases. The rise in panel temperature accompanying increased irradiance causes the bandgap of the semiconductor material to narrow, resulting in a logarithmic decrease in open-circuit voltage. These voltage losses resulting from the temperature increase cause a decrease in the power output per unit of irradiance. Consequently, since the input energy increases faster than the electrical output, energy efficiency decreases. As irradiance increases and the panel surface temperature rises relative to the ambient temperature, entropy production within the system increases, thereby increasing irreversibility (exergy loss). While solar radiation possesses a very high exergy potential from a thermodynamic perspective, the conversion of a significant portion of this potential into low-quality thermal energy due to the panel's heating is the primary factor in the decline of exergy efficiency. In summary, although the system generates more power under high irradiation, the utilization rate of the available exergy source (efficiency) decreases due to thermal losses and increased entropy.

If the energy efficiency exceeds the exergy efficiency under both low and high sunlight conditions, this can be explained by entropy generation and irreversibility. Internal resistances within the PV panel, and particularly the temperature increase on the panel's surface, lead to continuous entropy generation in the system. According to the second law of thermodynamics, every instance of entropy generation constitutes exergy destruction—that is, irreversibility. Even under low irradiance, the panel's interaction with the environment and optical losses can create irreversibility significant enough to reduce the system's potential to perform work below the level of electrical efficiency. Under high solar irradiance, the increase in panel temperature further increases exergy destruction, thereby maintaining the difference.

3.3 | Exergy Loss Coefficient and Energy–Exergy Efficiency as a Function of PV Panel Surface Temperature for Different Tilt

The dimensionless coefficient defines the loss caused by an increase in panel surface temperature relative to the input exergy

ijer, 2026, 1, Downloaded from https://onlinelibrary.wiley.com/doi/10.1155/er/1293591 by Hacer AKHAN - Trakya Universitesi , Wiley Online Library on [23/09/2026]. See the Terms and Conditions (https://onlinelibrary.wiley.com/terms-and-conditions) on Wiley Online Library for rules of use; OA articles are governed by the applicable Creative Commons License

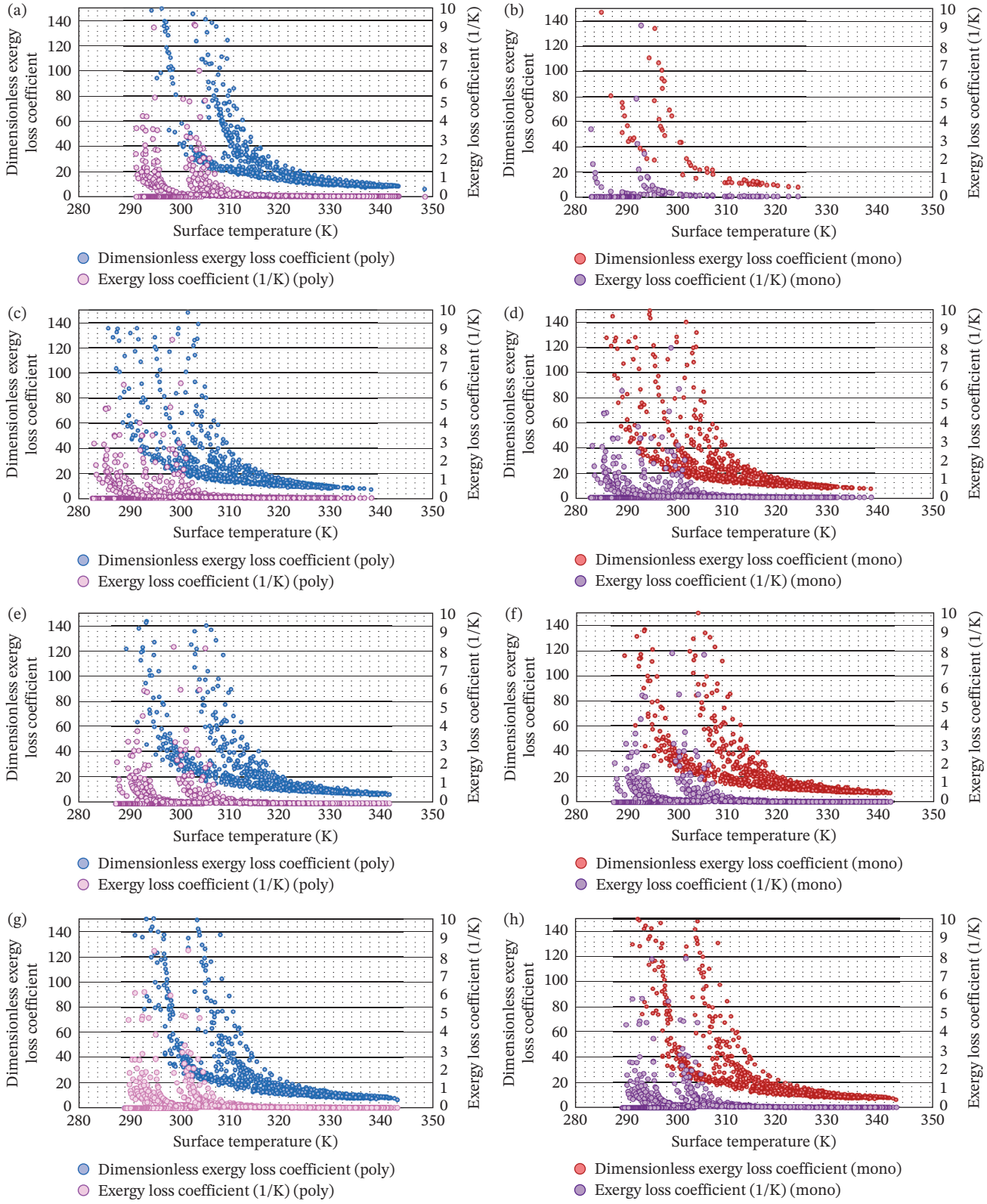


FIGURE 10 | (Continued)

ijer, 2026, 1, Downloaded from https://onlinelibrary.wiley.com/doi/10.1155/er/1293591 by Hacer AKHAN - Trakya Universitesi , Wiley Online Library on [23/09/2026]. See the Terms and Conditions (https://onlinelibrary.wiley.com/terms-and-conditions) on Wiley Online Library for rules of use; OA articles are governed by the applicable Creative Commons License

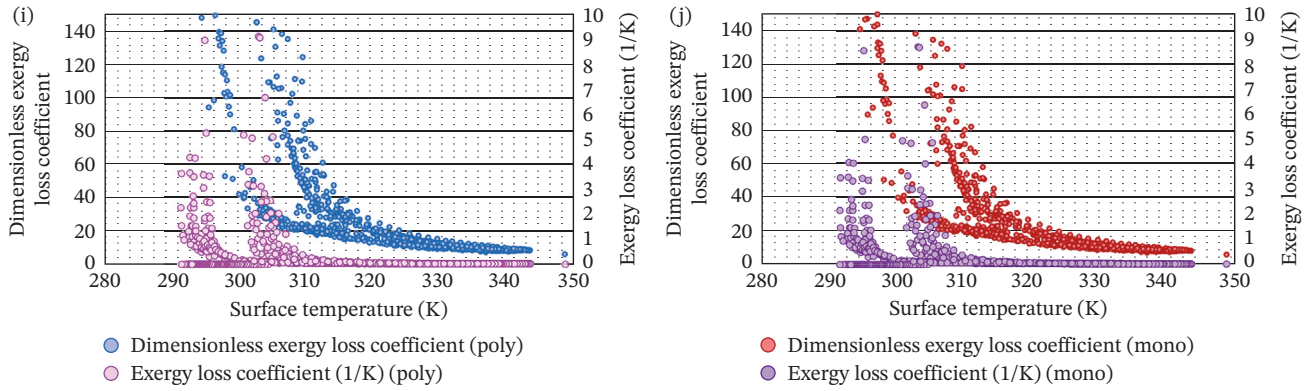


FIGURE 10 | Dimensionless exergy loss coefficient for polycrystalline and monocrystalline silicon PV panels with different tilts, and the variation of the exergy loss coefficient with surface temperature. (a) 0°, (b) 0°, (c) 10°, (d) 10°, (e) 20°, (f) 20°, (g) 30°, (h) 30°, (i) 40°, and (j) 40°.

based on the temperature difference normalized to the ambient temperature. This coefficient is a dimensionless performance indicator that reflects the panel's sensitivity to temperature increases.

The evaluation of the exergy loss coefficient related to surface temperature in PV panels has not been defined by a universal standard or critical value in the literature. This coefficient is a unique performance indicator showing the extent to which the panel's exergy efficiency is sensitive to changes in the surface temperature. Therefore, the interpretation of numerical values depends on the scope of the study and the analysis of the experimental data used.

In Figure 10a, a 0° tilted, in Figure 10c, a 10° tilted, in Figure 10e, a 20° tilted, in Figure 10g, a 30° tilted, and in Figure 10i, a 0° tilted polycrystalline PV panel; and in Figure 10b, a 40° tilted, in Figure 10d, a 10° tilted, in Figure 10f, a 20° tilted, in Figure 10h, a 30° tilted, and in Figure 10j, a 40° tilted monocrystalline PV panel, the variation of the dimensionless exergy loss coefficient and the exergy loss coefficient with surface temperature is presented. The numerical value of the dimensionless exergy coefficient for a PV panel, which depends on surface temperature, indicates how quickly the panel loses its exergy efficiency as the temperature rises. In other words, this value quantitatively expresses the panel's thermal sensitivity and performance durability. The point at which the tilt of the exergy loss coefficient changes or approaches a minimum is considered the critical temperature. The breakpoint is the critical temperature at which the temperature-dependent behavior of the coefficient changes. When the dataset is analyzed using breakpoint analysis with the Python programming language, the relationship between the dimensionless exergy loss coefficient and surface temperature shows a distinct break (change in slope) at approximately 308.15 and 218.15 K. According to analyses based on data obtained from experimental studies, the critical temperature for both panels falls within the range of 35–45°C (310.15–318.15 K). When the panel surface temperature exceeds this value, the exergy efficiency drops rapidly, and losses become irreversible. The fact that the exergy loss coefficient approaches its minimum after the critical temperature indicates that the panel's sensitivity to temperature decreases but absolute losses accelerate. For PV, the critical temperature is the threshold at which the panel's exergy efficiency begins to deteriorate rapidly. Within the critical temperature range, the dimensionless exergy loss coefficient for polycrystalline and monocrystalline silicon PV panels varies between 19 and 23. This value is higher for monocrystalline panels and lower for polycrystalline panels.

A low coefficient indicates that an increase in panel surface temperature has a limited effect on exergy loss and that the panel is more resistant to temperature increases. Conversely, a high coefficient indicates that even small temperature increases lead to significant exergy losses and that the panel is more sensitive to temperature increases. Therefore, the coefficient can be used as a "sensitivity metric" for evaluating the thermodynamic performance of PV systems.

A high coefficient indicates that the PV panel is highly sensitive to small temperature differences. Even minor temperature increases result in significant losses in the exergy efficiency. This demonstrates that the panel has a high marginal sensitivity to temperature. When the coefficient is low, the panel has already approached low efficiency levels at high temperature differences. Exergy losses still increase, but the relative response to temperature has weakened. This indicates that the panel's marginal sensitivity to temperature increases has decreased.

In Figure 11a, a 0° inclined polycrystalline PV panel; in Figure 11c, a 10° inclined panel; in Figure 11e, a 20° inclined panel; in Figure 11g, a 30° inclined panel; in Figure 11i, a 0° inclined panel; and in Figure 11b, a 40° inclined monocrystalline PV panel; in Figure 11d, a 10° inclined panel; in Figure 11f, a 20° inclined panel; in Figure 11h, a 30° inclined panel; and in Figure 11j, a 40° inclined monocrystalline PV panel, the variation of exergy loss and the dimensionless exergy loss coefficient with surface temperature is presented.

As the surface temperature of the PV panel increases, the output exergy decreases and exergy loss increases, this leads to an increase in the coefficient. On the other hand, as the temperature difference increases, the normalizing term $\left(\frac{T_0}{(T_S - T_0)}\right)$ decreases. This second effect reduces the value of the coefficient. This behavior reinforces the physical interpretation of the coefficient: while exergy loss appears more critical at low temperature differences, at high temperature differences, the loss is already a

ijer, 2026, 1, Downloaded from https://onlinelibrary.wiley.com/doi/10.1155/er/1293591 by Hacer AKHAN - Trakya Universitesi , Wiley Online Library on [23/09/2026]. See the Terms and Conditions (https://onlinelibrary.wiley.com/terms-and-conditions) on Wiley Online Library for rules of use; OA articles are governed by the applicable Creative Commons License

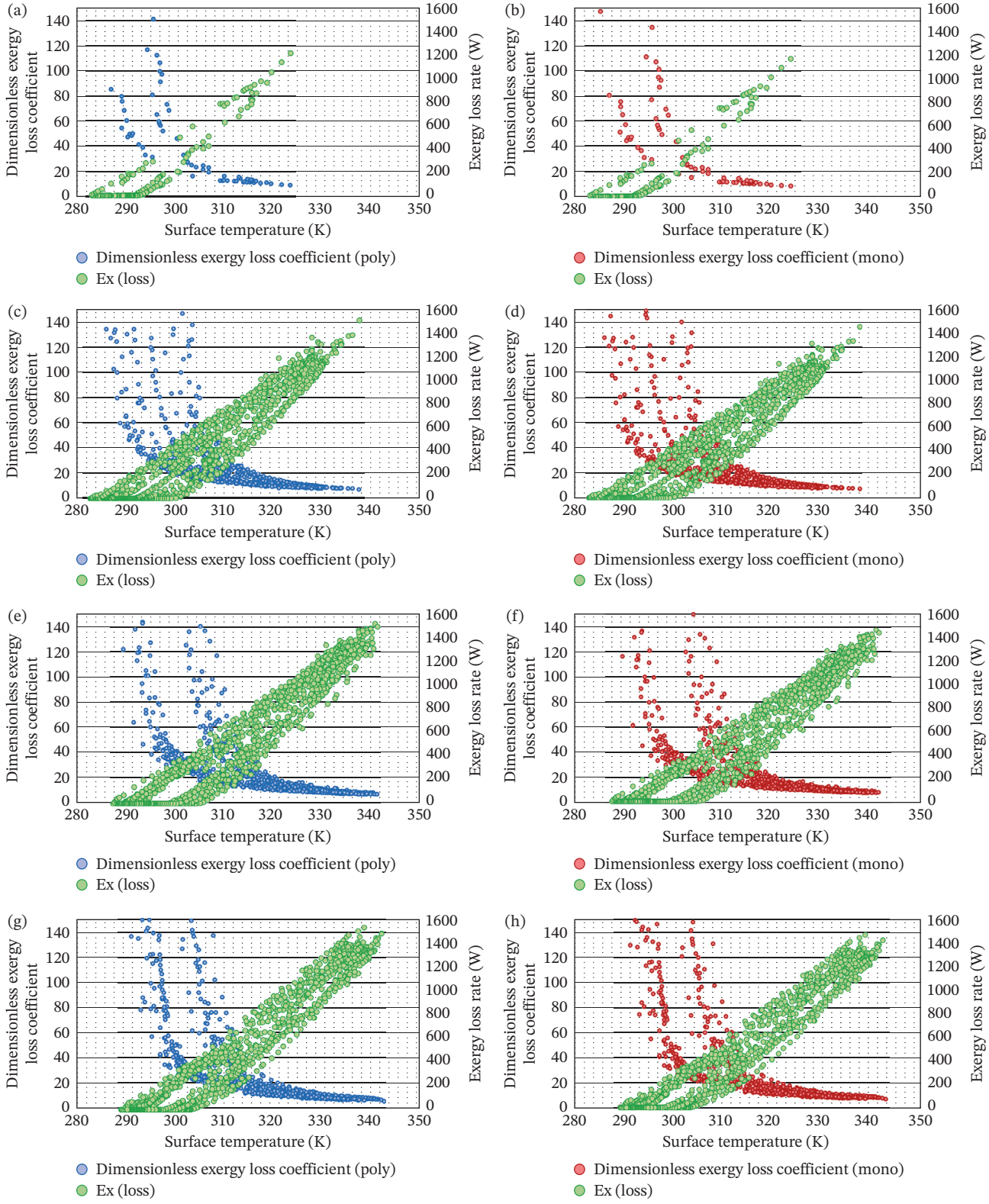


FIGURE 11 | (Continued)

ijer, 2026, 1, Downloaded from https://onlinelibrary.wiley.com/doi/10.1155/er/1293591 by Hacer AKHAN - Trakya Universitesi , Wiley Online Library on [23/09/2026]. See the Terms and Conditions (https://onlinelibrary.wiley.com/terms-and-conditions) on Wiley Online Library for rules of use; OA articles are governed by the applicable Creative Commons License

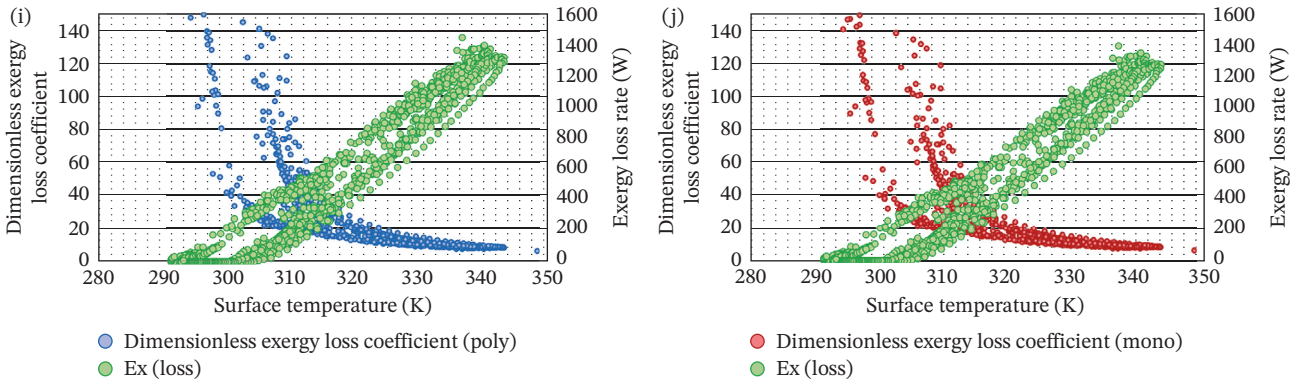


FIGURE 11 | Variation of exergy loss and dimensionless exergy loss coefficient for polycrystalline and monocrystalline silicon PV panels with different tilts as a function of surface temperature. (a) 0°, (b) 0°, (c) 10°, (d) 10°, (e) 20°, (f) 20°, (g) 30°, (h) 30°, (i) 40°, and (j) 40°.

natural consequence of the system, causing the coefficient to decrease to smaller values on a normalized scale. Thus, the coefficient presents the effect of surface temperature on exergy losses in a comparable and scalable manner. This feature provides a unique contribution that standardizes performance analysis across different climate conditions and panel types.

Figure 12a shows the 0° inclined, Figure 12c shows the 10° inclined, Figure 12e shows the 20° inclined, Figure 12g shows the 30° inclined, and Figure 12i shows the 0° inclined polycrystalline PV panel; while Figure 12b shows the 40° inclined, Figure 12d shows the 10° inclined, Figure 12f shows the 20° inclined, Figure 12h shows the 30° inclined, and Figure 12j shows the 40° inclined monocrystalline PV panel, illustrating the variation of energy–exergy efficiency and the dimensionless exergy loss coefficient with surface temperature. As the surface temperature increases, the energy and exergy efficiency of the PV panel decrease. The exergy loss coefficient changes in proportion to the exergy efficiency because the coefficient represents the relative sensitivity to the temperature increase. In panels with a high initial efficiency, the coefficient is higher, whereas in those with a low efficiency, it is lower.

Figure 13a shows a polycrystalline silicon PV panel with a 0° tilt, Figure 13c shows a 10° tilt, Figure 13e shows a 20° tilt, Figure 13g shows a 30° tilt, and Figure 13i shows a 40° tilt; Figure 13b shows a monocrystalline silicon PV panel with a 0° tilt, Figure 13d shows a 10° tilt, Figure 13f shows a 20° tilt, Figure 13h shows a 30° tilt, and Figure 13j shows a 40° tilt, presenting the variation of exergy efficiency and exergy loss rate with surface temperature. Exergy efficiency measures not only the amount of energy produced but also the usability of this energy. As the surface temperature increases, entropy generation and irreversibility increase; this reduces the system's capacity to produce ordered energy. Therefore, the exergy efficiency decreases more rapidly than the energy efficiency. The exergy loss rate indicates the rate at which irreversibility in the panel increases with rising temperature. At high temperatures, carrier recombination, radiation, and conduction losses occur more intensely, causing the exergy loss rate to rise. This indicates that the system becomes thermodynamically less efficient and that the potential for usable energy decreases rapidly.

For a 30° tilt, Figure 14a shows the variation over a 1-day period of the energy–exergy efficiencies and the dimensionless exergy loss coefficient of the polycrystalline PV panel, and Figure 14b shows the energy–exergy efficiencies and the dimensionless exergy loss coefficient of the monocrystalline PV panel.

For a 30° tilt, the variation over a 1-day time period of the incoming exergy rate, exergy loss rate, and dimensionless exergy loss coefficient of the polycrystalline silicon PV panel shown in Figure 15a and the incoming exergy rate, exergy loss rate, and dimensionless exergy loss coefficient of the monocrystalline silicon PV panel shown in Figure 15b, is presented.

In Figure 16a, 0° inclined; in Figure 16b, 10° inclined; in Figure 16c, 20° inclined; in Figure 16d, 30° inclined; and in Figure 16e, 40° inclined polycrystalline and monocrystalline silicon PV panels, the variation of the dimensionless exergy loss coefficient with surface temperature is shown.

The primary reason why the exergy loss coefficient in monocrystalline silicon PV panels is lower than that in polycrystalline panels is related to the crystalline order and carrier mobility in the material structure. Monocrystalline silicon: It has a single-crystal structure. Electrons encounter fewer obstacles within the crystal lattice, and carrier losses are limited. Thanks to this ordered structure, the exergy efficiency degrades less in response to temperature increases. Polycrystalline silicon consists of a combination of numerous crystalline grains. Electron movement becomes more difficult at grain boundaries, and recombination losses increase. Therefore, temperature increases reduce the exergy efficiency to a greater extent.

The exergy loss coefficient measures the relative sensitivity to temperature increases. Since monocrystalline panels have a higher initial efficiency, the loss caused by temperature increases is relatively lower, resulting in a smaller coefficient. In polycrystalline panels, the initial efficiency is lower, and the effect of temperature is more pronounced, so the loss is relatively greater, resulting in a higher coefficient. This difference indicates that monocrystalline panels are more resistant to temperature increases. A low coefficient indicates that the panel better maintains its exergy efficiency in the face of changes in the surface temperature. Polycrystalline panels, on the other hand, are more sensitive to temperature increases because they have a higher coefficient.

ijer, 2026, 1, Downloaded from https://onlinelibrary.wiley.com/doi/10.1155/er/1293591 by Hacer AKHAN - Trakya Universitesi , Wiley Online Library on [23/09/2026]. See the Terms and Conditions (https://onlinelibrary.wiley.com/terms-and-conditions) on Wiley Online Library for rules of use; OA articles are governed by the applicable Creative Commons License

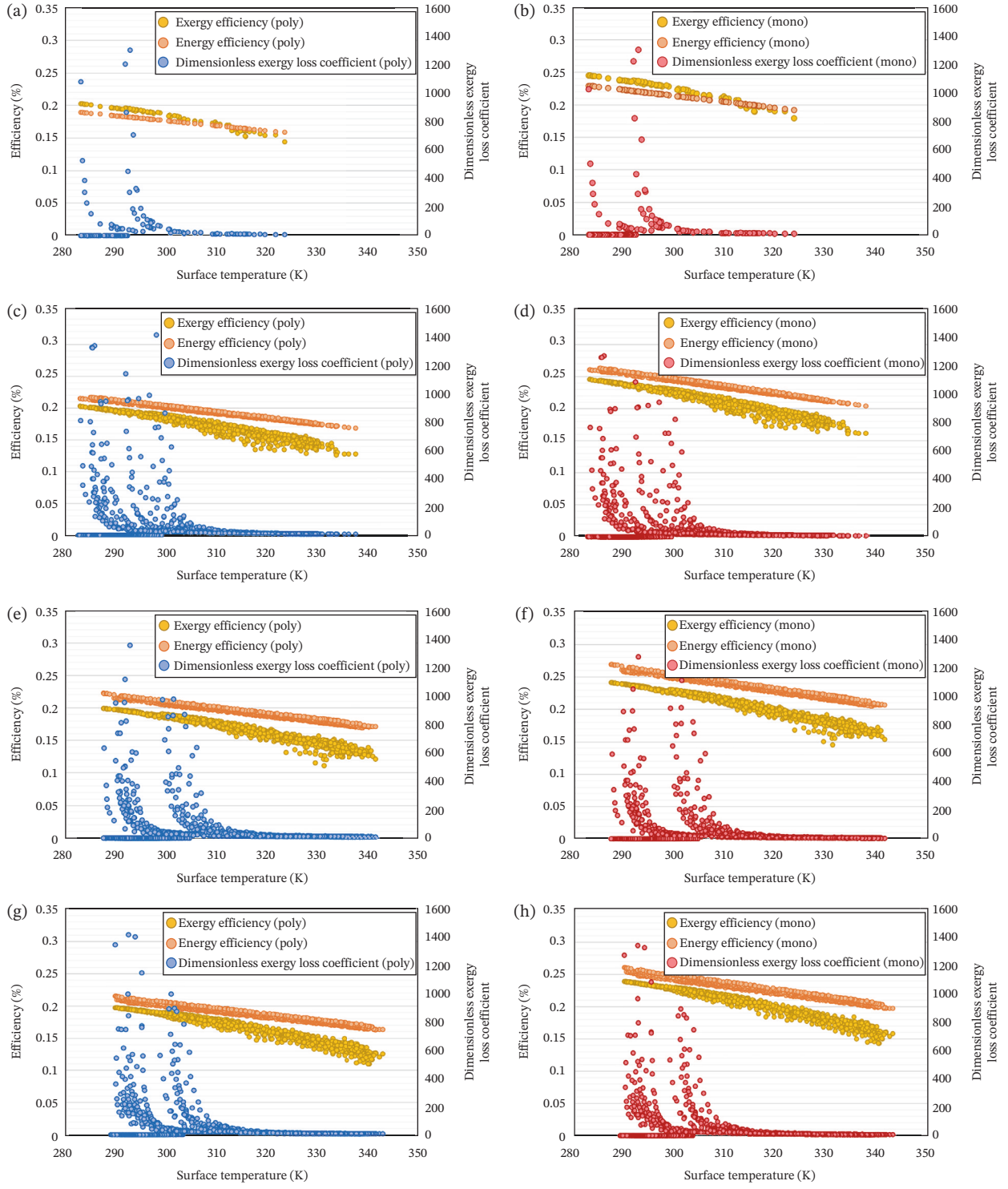


FIGURE 12 | (Continued)

ijer, 2026, 1, Downloaded from https://onlinelibrary.wiley.com/doi/10.1155/er/1293591 by Hacer AKHAN - Trakya Universitesi , Wiley Online Library on [23/09/2026]. See the Terms and Conditions (https://onlinelibrary.wiley.com/terms-and-conditions) on Wiley Online Library for rules of use; OA articles are governed by the applicable Creative Commons License

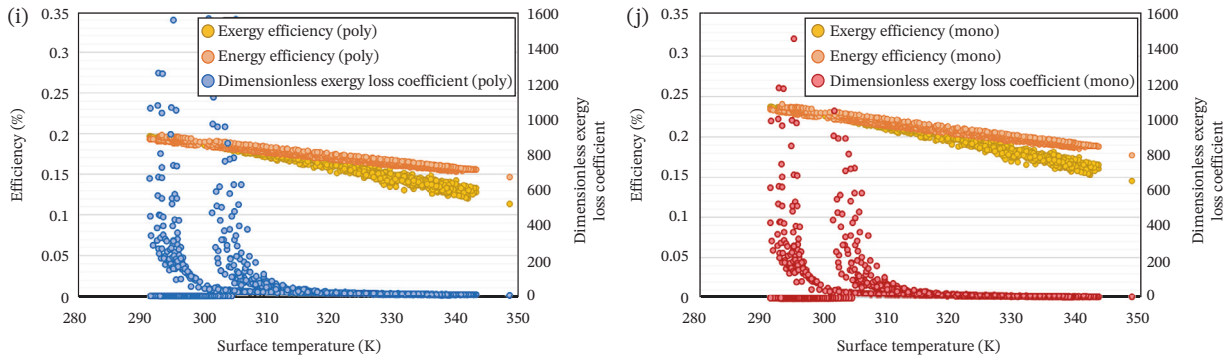


FIGURE 12 | Variation of energy–exergy efficiency and dimensionless exergy loss coefficient of polycrystalline and monocrystalline silicon PV panels with different tilts as a function of surface temperature. (a) 0°, (b) 0°, (c) 10°, (d) 10°, (e) 20°, (f) 20°, (g) 30°, (h) 30°, (i) 40°, and (j) 40°.

The reason the exergy loss coefficient is lower in monocrystalline silicon PV panels compared to polycrystalline ones is that carrier losses are limited due to the regularity of the crystal structure, and the exergy efficiency is less degraded by temperature increases.

3.4 | Evaluation of the Multiple Regression Model

In this study, a multiple regression model was used to simultaneously examine the effects of multiple independent variables on the dimensionless exergy loss coefficient, which depends on the surface temperature of PV panels. The objective was to identify the most significant physical and environmental effects on the coefficient and to develop a prediction model. The model was analyzed in Python and Excel environments; the significance of the coefficients and the model's coefficient of determination (R^2) were calculated. Equations (25)–(27) present the energy efficiency multiple regression model. The purpose of the regression model is to estimate the exergy loss coefficient of the PV panel system as a function of the surface temperature. The PV panel surface temperature T_S has been considered equal to the module temperature T_m in the calculations.

Dependent variables are as follows:

$\theta^*_{T_S}(X_i) =$ Exergy loss coefficient (dimensionless) for $T_S < 35°C$.

$\theta^*_{T_S}(X_i) =$ Exergy loss coefficient (dimensionless) for $45°C \geq T_S \geq 35°C$.

$\theta^*_{T_S}(X_i) =$ Exergy loss coefficient (dimensionless) for $T_S > 45°C$.

Subscript i defines the independent variables from 1 to 6.

Independent variables (inputs) are as follows:

$X_1 =$ PV panel type (monocrystalline = 0, polycrystalline = 1) [dummy variable].

$X_2 =$ Ambient temperature (°C).

$X_3 =$ Wind speed (m/s).

$X_4 =$ Solar radiation (W/m^2).

$X_5 =$ PV panel surface temperature (°C).

$X_6 =$ PV panel tilt (°).

In regression analyses, categorical variables, such as panel type, must be converted into a numerical data format. When there are two different PV panel types, namely, monocrystalline and polycrystalline, defining a single dummy variable is sufficient to include this variable in the model. If the monocrystalline panel type is taken as the reference group, the coding is performed as follows:

- Monocrystalline silicon → $X_1 = 0$.
- Polycrystalline silicon → $X_1 = 1$.

For surface temperatures below 35°C, the model for the dimensionless exergy loss coefficient $\theta^*_{T_S}$, which depends on surface temperature, is given in Equation (16). The expression for $\theta^*_{T_S}$ in Equation (17) includes the values of all independent variables.

$$\theta^*_{T_S}(X_i) = a_0 + a_1X_1 + a_2X_2 + a_3X_3 + a_4X_4 + a_5X_5 + a_6X_6 + \varepsilon \text{ for } T_S < 35°C, \tag{16}$$

$$\theta^*_{T_S}(X_i) = 61.61781974 + 3.964257442 \times X_1 + 3.441456009 \times X_2 + 0.223040307 \times X_3 - 0.008532854 \times X_4 - 3.373025101 \times X_5 - 0.077815624 \times X_6 \text{ for } T_S < 35°C. \tag{17}$$

ijer, 2026, 1, Downloaded from https://onlinelibrary.wiley.com/doi/10.1155/er/1293591 by Hacer AKHAN - Trakya Universitesi , Wiley Online Library on [23/09/2026]. See the Terms and Conditions (https://onlinelibrary.wiley.com/terms-and-conditions) on Wiley Online Library for rules of use; OA articles are governed by the applicable Creative Commons License

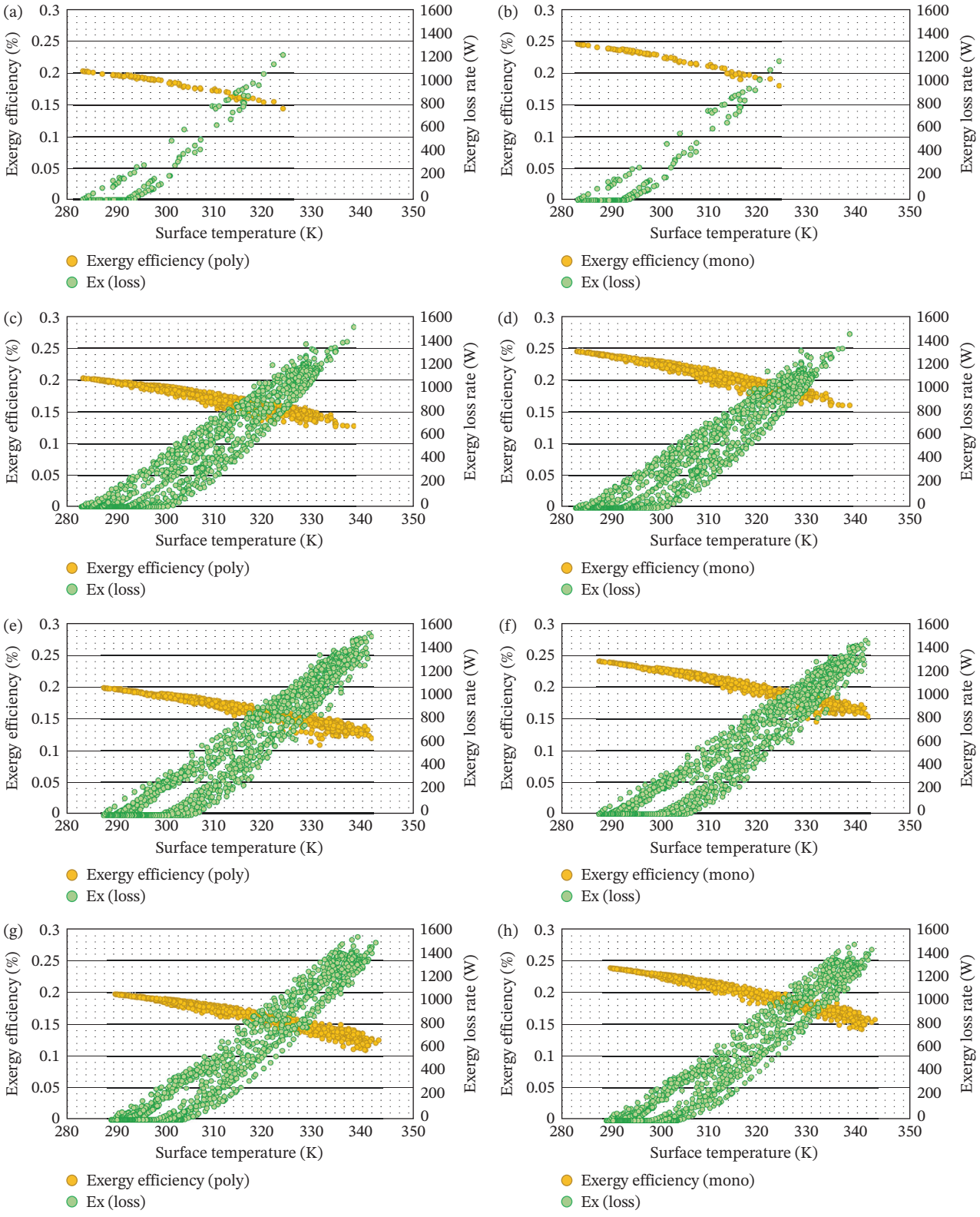


FIGURE 13 | (Continued)

ijer, 2026, 1, Downloaded from https://onlinelibrary.wiley.com/doi/10.1155/er/1293591 by Hacer AKHAN - Trakya Universitesi , Wiley Online Library on [23/09/2026]. See the Terms and Conditions (https://onlinelibrary.wiley.com/terms-and-conditions) on Wiley Online Library for rules of use; OA articles are governed by the applicable Creative Commons License

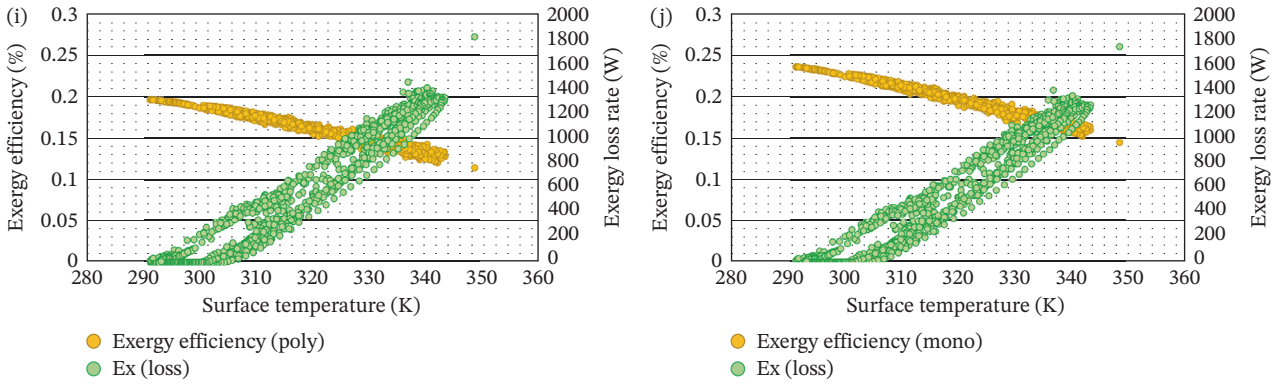


FIGURE 13 | Variation of exergy efficiency and exergy loss rate of polycrystalline and monocrystalline silicon PV panels with different tilts as a function of surface temperature. (a) 0°, (b) 0°, (c) 10°, (d) 10°, (e) 20°, (f) 20°, (g) 30°, (h) 30°, (i) 40°, and (j) 40°.

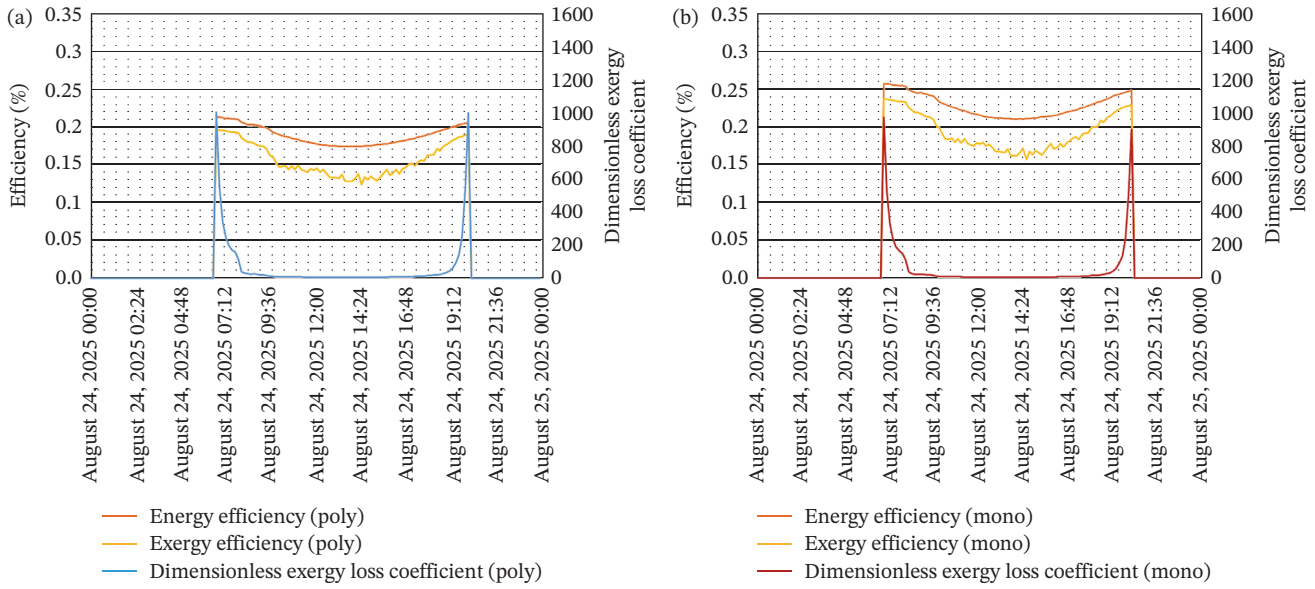


FIGURE 14 | Changes in the energy–exergy efficiencies of polycrystalline and monocrystalline PV panels at a 30° tilt and in the dimensionless exergy loss coefficient over a 24 h period. (a) 30° and (b) 30°.

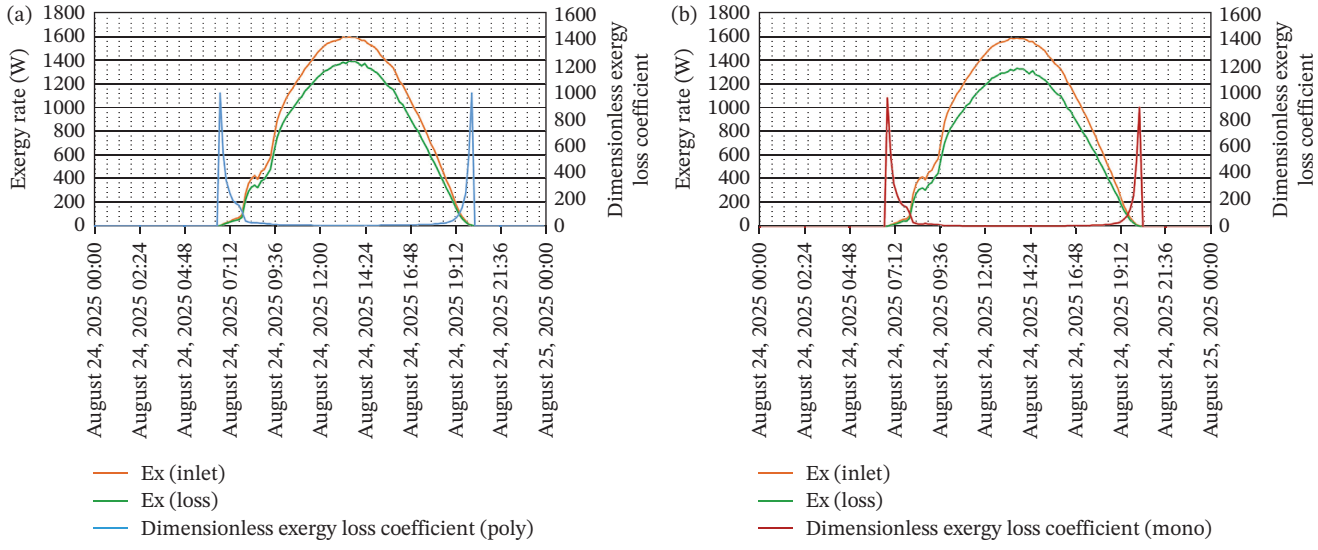


FIGURE 15 | Variation in the exergy input rate, exergy loss rate, and dimensionless exergy loss coefficient of polycrystalline and monocrystalline silicon PV panels tilted at 30° over a 24 h period. (a) 30° and (b) 30°.

ijer, 2026, 1, Downloaded from https://onlinelibrary.wiley.com/doi/10.1155/er/1293591 by Hacer AKHAN - Trakya Universitesi , Wiley Online Library on [23/09/2026]. See the Terms and Conditions (https://onlinelibrary.wiley.com/terms-and-conditions) on Wiley Online Library for rules of use; OA articles are governed by the applicable Creative Commons License

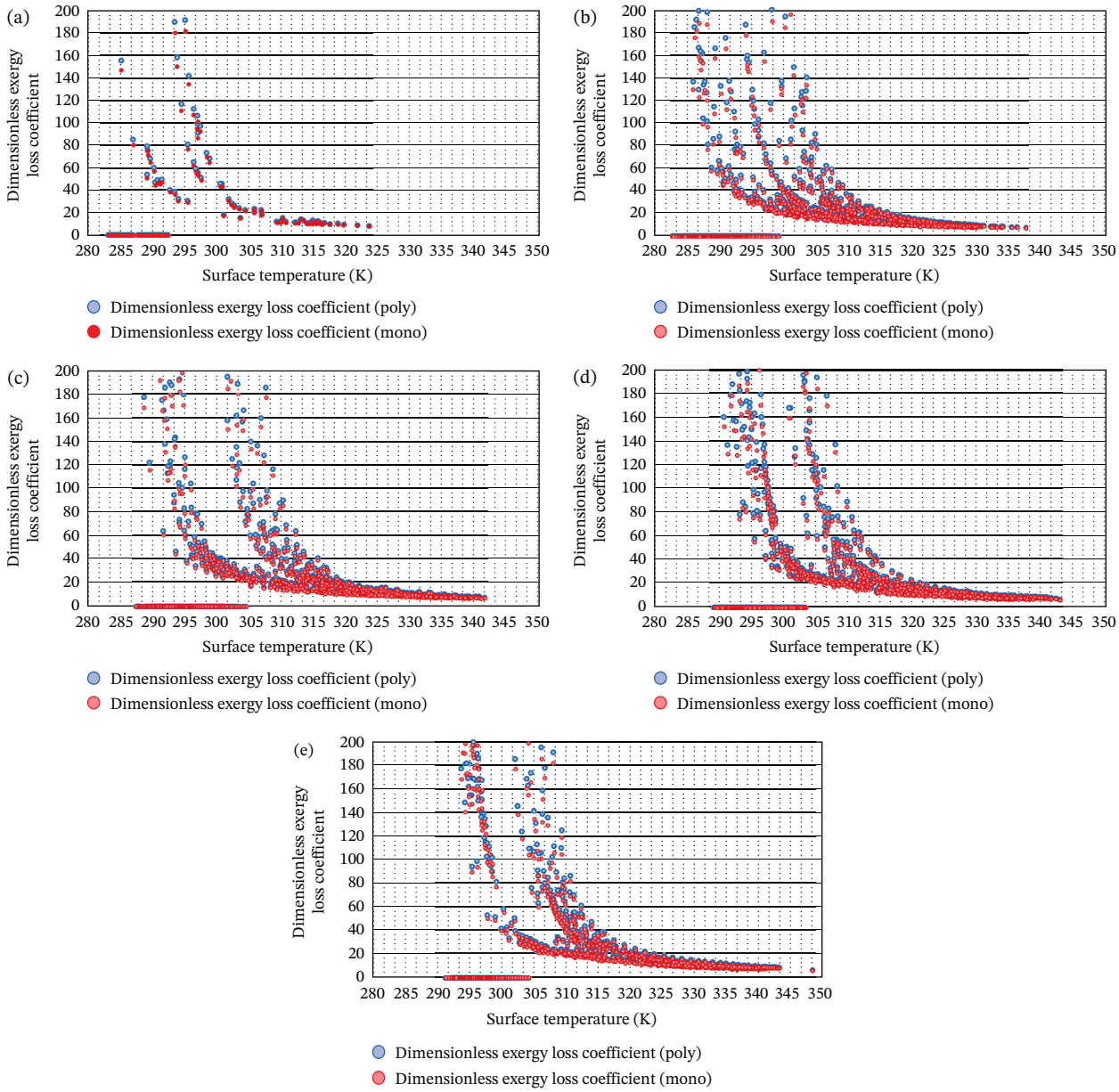


FIGURE 16 | Variation of the dimensionless exergy loss coefficient of polycrystalline and monocrystalline silicon PV panels with surface temperature for different tilts. (a) 0°, (b) 10°, (c) 20°, (d) 30°, and (e) 40°.

Table 9 presents the results of the multiple regression analysis for the exergy loss coefficient when T_S <35°C. The coefficients show the effect of the variables, the standard error shows the reliability, the *t*-statistic (*t*-Stat) and *p*-value indicate significance, and the confidence intervals show the possible range of the coefficient. The coefficients represent the estimated effect of the independent variable on the dependent variable. A positive coefficient indicates that an increase in the variable increases the dependent variable, while a negative coefficient indicates that it decreases it. Standard error measures the uncertainty in the coefficient estimate. It takes values starting from 0 and is non-negative. Being close to 0 increases the reliability of the coefficient; as it increases, the uncertainty of the coefficient also increases. The *t*-stat tests whether the coefficient is significantly different from zero. It is calculated using the formula coefficient/standard error. The *p*-value shows whether the coefficient is statistically significant. It is generally considered significant if it is below 0.05 (meaning the hypothesis is rejected). The lower 95% and upper 95% (confidence interval) indicate the 95% confidence interval of the coefficient. This range shows the bounds within which the true value of the coefficient is expected to lie with a 95% probability. In regression analysis, the confidence intervals obtained are crucial for evaluating the statistical significance of the coefficients and the reliability of the model. For the intercept, the interval [60.09; 63.15] is relatively narrow and does not include zero, indicating that the constant term is highly significant with a strong level of confidence. For X_1, the interval [−0.59; 8.52] includes zero, suggesting that the effect of this variable is not statistically significant and that the coefficient may either be positive or negligible. In contrast, the interval [2.84; 4.04] for X_2 is narrow and excludes zero, confirming a strong and significant positive effect. The intervals [−3.97; −2.78] for X_5 and [−0.100;

ijer, 2026, 1, Downloaded from https://onlinelibrary.wiley.com/doi/10.1155/er/1293591 by Hacer AKHAN - Trakya Universitesi , Wiley Online Library on [23/09/2026]. See the Terms and Conditions (https://onlinelibrary.wiley.com/terms-and-conditions) on Wiley Online Library for rules of use; OA articles are governed by the applicable Creative Commons License

TABLE 9 | Exergy loss coefficient for T_S <35°C: multiple regression analysis results.

Intercept, independent variables	Coefficient (a_i)	Standard error	*t*-Stat	*p*-Value	Lower 95%	Upper 95%
Intercept	61.61781974	0.779509303	79.04693316	0	60.08861375	63.14702573
X_1	3.964257442	2.320335445	1.708484629	0.087780485	−0.587671369	8.516186254
X_2	3.441456009	0.305926553	11.24928835	4.18123E-28	2.841303176	4.041608842
X_3	0.223040307	0.166006076	1.343567128	0.179318276	−0.102622882	0.548703497
X_4	−0.008532854	0.010844599	−0.786829885	0.431522057	−0.029807296	0.012741587
X_5	−3.373025101	0.304392253	−11.08117919	2.35661E − 27	−3.970168014	−2.775882188
X_6	−0.077815624	0.011404579	−6.823191434	1.35031E − 11	−0.100188609	−0.055442639

TABLE 10 | Regression statistics for exergy loss coefficient at T_S <35°C.

Regression statistics	
Multiple R	0.932451507
R^2	0.869465813
Adjusted R^2	0.868875161
Standard error (RMSE)	3.979853274
MAE	3.98
Observations	1333

−0.055] for X_6 are both narrow and exclude zero, demonstrating that these variables exert strong and statistically significant negative effects.

In regression analysis, the regression statistics for the exergy loss coefficient at T_S <35°C values, used to evaluate the overall goodness of fit of the model, are shown in Table 10. Multiple R is the correlation coefficient between the dependent variable and the values predicted by the model. It ranges between 0 and 1; values close to 0 indicate a weak relationship, while values close to 1 indicate a strong linear relationship. R^2 shows how much of the total variance in the dependent variable is explained by the model. It ranges between 0 and 1. Values between 0.10 and 0.30 are interpreted as low, 0.30–0.50 as moderate, and 0.50 and above as high explanatory power. Adjusted R^2 is the R^2 value corrected according to the number of independent variables. R^2 can increase artificially when unnecessary variables are added to the model; adjusted R^2 balances this situation and provides a more realistic measurement. The closeness of adjusted R^2 to R^2 indicates the robustness of the model. Standard error expresses the average magnitude of the model's prediction error. It takes positive values starting from 0. A small standard error indicates that the model's predictions are closer to the observations, while large values indicate low reliability of the predictions. Observation refers to the number of data points included in the analysis.

Table 11 presents the ANOVA test results for T_S <35°C. In the ANOVA table, df indicates the degrees of freedom, sum of squares (SS) the total variance, MS the mean variance, *F* the magnitude of the difference between groups, and significance *F* reveals whether this difference is statistically significant. df shows the amount of independent information used in the calculation of variance. SS is the total deviation measure, indicating the source of variance. MS is obtained by dividing the SS value by the relevant df. The between-groups MS represents the average variance between groups, while the within groups MS represents the error variance. *F* (*F*-statistic) is the ratio of the between-groups MS to the within-groups MS. The larger this ratio is, the more likely the difference between groups is considered meaningful rather than random. Significance *F* (*p*-value) indicates the statistical significance of the *F*-statistic. It takes values between 0 and 1. Generally, a value below 0.05 indicates that there is a significant difference between the groups. According to Table 11, the *F*-value of 1472.04 is remarkably high, indicating that the independent variables collectively exert a strong explanatory effect on the dependent variable. Furthermore, the significance $F = 0$ (practically $p < 0.0001$) confirms that the model is statistically highly significant. These findings validate, at an academic level, that the constructed regression model is both reliable and explanatory in nature. The RMSE value indicates that the average magnitude of error between the model's predictions and the actual values is approximately 4 units. In other words, the model estimates the observations with an average deviation of about ±4. The smaller this value is, the more reliable the model's predictions become. The MAE value, on the other hand, represents the mean of the absolute differences. Thus, the average absolute error between the predicted and actual values is 3.98. The fact that the RMSE is only slightly larger than MAE suggests that the

TABLE 11 | ANOVA test results for T_S <35°C.

ANOVA	df	SS	MS	*F*	Significance *F*
Regression	6	139,896.1905	23,316.03175	1472.043065	0
Difference	1326	21,002.82174	15.83923208	—	—
Total	1332	160,899.0122	—	—	—

ijer, 2026, 1, Downloaded from https://onlinelibrary.wiley.com/doi/10.1155/er/1293591 by Hacer AKHAN - Trakya Universitesi , Wiley Online Library on [23/09/2026]. See the Terms and Conditions (https://onlinelibrary.wiley.com/terms-and-conditions) on Wiley Online Library for rules of use; OA articles are governed by the applicable Creative Commons License

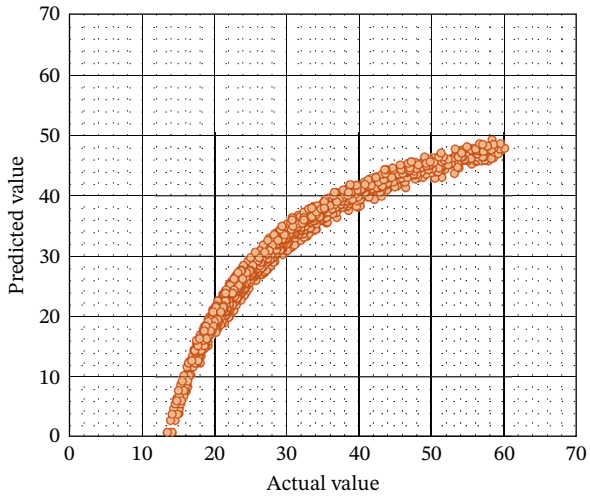


FIGURE 17 | Actual and predicted values for energy efficiency multivariate regression for T_S <35°C.

Figure 17 shows the actual and predicted values for energy efficiency multivariate regression. The actual and predicted values diagram visually reveals how closely the model's predictions align with the true values. If the points cluster around the $y=x$ line, the model is strong; as deviations and dispersion increase, the model's reliability decreases. Predictions closely follow the true values at low values, while the deviation increases at higher values. This indicates that there may be a nonlinear relationship between the dependent and independent variables. Figure 18 shows the difference between actual and estimated values for the exergy loss coefficient.

For surface temperatures below 45°C ≥ T_S ≥ 35°C, the model for the dimensionless exergy loss coefficient $\theta^*_{T_S}$, which depends on surface temperature, is given in Equation (18). The expression for $\theta^*_{T_S}$ in Equation (19) includes the values of all independent variables.

error distribution does not contain extreme outliers and that the model provides balanced predictions.

$$\theta^*_{T_S}(X_i) = b_0 + b_1X_1 + b_2X_2 + b_3X_3 + b_4X_4 + b_5X_5 + b_6X_6 + \varepsilon'' \text{ for } 45°C \geq T_S \geq 35°C, \tag{18}$$

$$\theta^*_{T_S}(X_i) = 32.22639288 + 1.046058005 \times X_1 + 1.795356109 \times X_2 + 0.01663864 \times X_3 + 0.0110484 \times X_4 - 1.584658016 \times X_5 - 0.037087649 \times X_6 \text{ for } 45°C \geq T_S \geq 35°C. \tag{19}$$

Table 12 shows the results of the multiple regression analysis for energy efficiency for 45°C ≥ T_S ≥ 35°C. When all independent variables are zero, the initial value of the dependent variable is approximately 32.2. When $X_1=1$ (polycrystalline silicon material), the average value of the dependent variable is approximately 1.05 units higher compared to $X_1=0$ (monocrystalline silicon material). In other words, this coefficient indicates the additional effect that switching to the relevant category has on the dependent variable. Increases in X_2, X_3, and X_4 indicate a positive and significant effect on the dimensionless exergy loss coefficient. Increases in X_5 and X_6 lead to a decrease in the dependent variable. In this regression analysis, the confidence intervals are critical for assessing the significance of the coefficients. For the intercept, the interval [30.93; 33.52] is narrow and does not include zero, indicating that the constant term is highly significant with strong confidence. For X_1, the interval [0.29; 1.81] excludes zero, demonstrating a statistically significant positive effect. The interval [1.66; 1.93] for X_2 is very narrow and excludes zero, confirming a strong and reliable positive effect. For X_4, the interval [0.0065; 0.0156] excludes zero, indicating a meaningful positive contribution. The interval [−1.72; −1.45] for X_5 is narrow and excludes zero, showing a strong and significant negative effect. Finally, the interval [−0.046; −0.028] for X_6 also excludes zero, confirming a statistically significant negative effect.

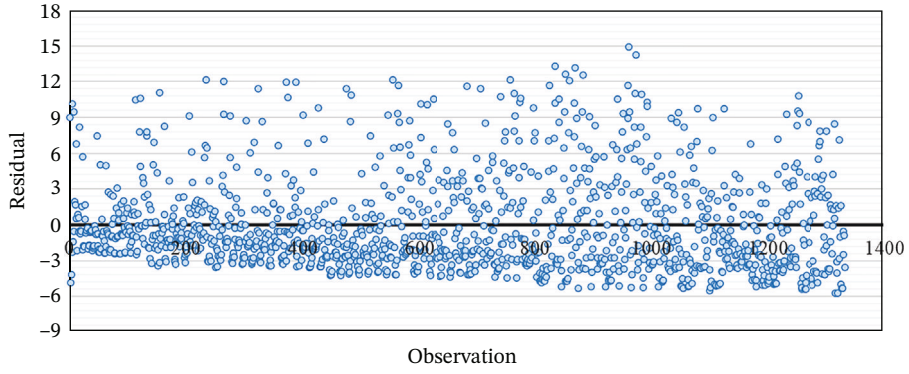


FIGURE 18 | The difference between actual and estimated values for exergy loss coefficient for T_S <35°C.

ijer, 2026, 1, Downloaded from https://onlinelibrary.wiley.com/doi/10.1155/er/1293591 by Hacer AKHAN - Trakya Universitesi , Wiley Online Library on [23/09/2026]. See the Terms and Conditions (https://onlinelibrary.wiley.com/terms-and-conditions) on Wiley Online Library for rules of use; OA articles are governed by the applicable Creative Commons License

TABLE 12 | Energy efficiency multiple regression analysis results for $45°C \geq T_S \geq 35°C$.

Intercept, independent variables	Coefficient (b_i)	Standard error	*t*-Stat	*p*-Value	Lower 95%	Upper 95%
Intercept	32.22639288	0.658742746	48.92105918	0	30.93436201	33.51842374
X_1	1.046058005	0.387574789	2.698983618	0.007023952	0.285884793	1.806231217
X_2	1.795356109	0.066960774	26.81205728	2.1568E − 132	1.664022007	1.926690211
X_3	0.01663864	0.065272993	0.254908491	0.798824574	−0.111385117	0.144662397
X_4	0.0110484	0.002299586	4.80451629	1.68752E − 06	0.006538086	0.015558713
X_5	−1.584658016	0.06652744	−23.81961517	1.8078E − 108	−1.715142194	−1.454173838
X_6	−0.037087649	0.004733468	−7.835195962	8.18041E − 15	−0.046371677	−0.02780362

TABLE 13 | Regression statistics of the exergy loss coefficient for $45°C \geq T_S \geq 35°C$.

Regression statistics	
Multiple R	0.952420561
R^2	0.907104924
Adjusted R^2	0.906777445
Standard error (RMSE)	1.868502076
MAE	1.91
Observations	1709

For $45°C \geq T_S \geq 35°C$, Table 13 contains the regression statistics of the exergy loss coefficient, and Table 14 presents the results of the ANOVA test. For a multiple R value of 0.95, there is a very high correlation between actual values and predicted values. The model explains 91% of the variance in the dependent variable. This is a very high explanatory power. Adjusted R^2 is very close to R^2. This indicates that the independent variables added to the model truly contribute to the model. The average magnitude of the prediction errors is approximately 1.9 units. When compared to the scale of the dependent variable, if this error is low, the model's predictions are considered reliable. A total of 1709 observations represent a very large sample size. This increases the statistical power and supports the reliability of the results. The model has very high explanatory power and shows strong correlation, and the results are statistically robust thanks to the large sample size. The standard error is also at a reasonable level. The F-test results obtained in this regression analysis evaluate the overall significance of the model. According to the table, the F-value of 2769.96 is remarkably high, indicating that the independent variables collectively have a strong explanatory effect on the dependent variable. Furthermore, the significance $F = 0$ (practically $p < 0.0001$) demonstrates that the model is statistically highly significant. These findings confirm, at an academic level, that the constructed regression model is both reliable and explanatory in nature. RMSE is slightly smaller than the MAE. This indicates that the error distribution is very balanced and that there are not many outliers.

Figure 19 shows the actual and predicted values for energy efficiency multivariate regression. Figure 20 shows the difference between the actual and estimated values for the exergy loss coefficient. While the predictions closely follow the actual values at low levels, the deviation increases at higher values.

For surface temperatures higher than 45°C, the model for the dimensionless exergy loss coefficient $\theta^*_{T_S}$, which depends on surface temperature, is given in Equation (20). The expression for $\theta^*_{T_S}$ in Equation (21) includes the values of all independent variables.

$$\theta^*_{T_S}(X_i) = c_0 + c_1X_1 + c_2X_2 + c_3X_3 + c_4X_4 + c_5X_5 + c_6X_6 + \varepsilon''' \text{ for } T_S > 45°C, \tag{20}$$

$$\theta^*_{T_S}(X_i) = 19.10176975 + 0.194071241 \times X_1 + 0.458984586 \times X_2 + 0.100335053 \times X_3 - 0.003986937 \times X_4 - 0.358311658 \times X_5 + 0.007992118 \times X_6 \text{ for } T_S > 45°C. \tag{21}$$

TABLE 14 | ANOVA test results for $45°C \geq T_S \geq 35°C$.

ANOVA	df	SS	MS	*F*	Significance *F*
Regression	6	58,024.52	9670.753334	2769.957699	0
Difference	1702	5942.192612	3.491300007	—	—
Total	1708	63,966.71262	—	—	—

ijer, 2026, 1, Downloaded from https://onlinelibrary.wiley.com/doi/10.1155/er/1293591 by Hacer AKHAN - Trakya Universitesi , Wiley Online Library on [23/09/2026]. See the Terms and Conditions (https://onlinelibrary.wiley.com/terms-and-conditions) on Wiley Online Library for rules of use; OA articles are governed by the applicable Creative Commons License

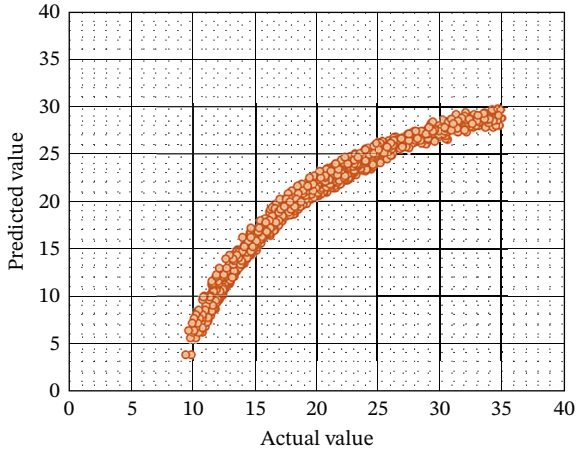


FIGURE 19 | Actual and predicted values for energy efficiency multivariate regression for 45°C ≥ T_S ≥ 35°C.

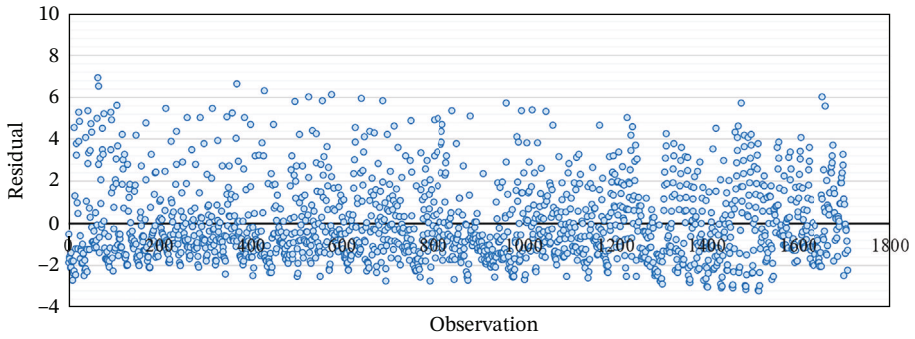


FIGURE 20 | The difference between actual and estimated values for energy efficiency for 45°C ≥ T_S ≥ 35°C.

Table 15 shows the results of the energy efficiency multiple regression analysis for T_S >45°C. When $X_1 = 1$, which represents the polycrystalline silicon material, the mean value of the dependent variable is approximately 0.19 units higher compared to $X_1 = 0$ (monocrystalline silicon). In other words, this coefficient indicates the additional effect of switching to the relevant category on the dependent variable. Increases in X_2, X_3, and X_6 indicate a positive and significant effect on the dimensionless exergy loss coefficient. Increases in X_4 and X_5 lead to a decrease in the dependent variable. In this regression analysis, the confidence interval for the intercept [18.83; 19.37] is narrow and does not include zero, indicating that the constant term is highly significant with a strong level of confidence. For X_2, the interval [0.43; 0.49] is also narrow and excludes zero, confirming a strong and reliable positive effect. The interval [0.058; 0.143] for X_3 does not include zero, demonstrating that this variable provides a statistically significant positive contribution. For X_4, the interval [−0.0050; −0.0029] is narrow and excludes zero, indicating a significant negative effect. Similarly, the interval [−0.388; −0.329] for X_5 is narrow and excludes zero, showing a strong and significant negative effect. Finally, the interval [0.0042; 0.0117] for X_6 excludes zero, confirming a statistically significant positive contribution.

For T_S >45°C, Table 16 presents the regression statistics of the exergy loss coefficient, and Table 17 presents the results of the

TABLE 15 | Energy efficiency multiple regression analysis results for T_S >45°C.

Intercept, independent variables	Coefficient (c_i)	Standard error	*t*-Stat	*p*-Value	Lower 95%	Upper 95%
Intercept	19.10176975	0.137255818	139.1691082	0	18.8326775	19.37086201
X_1	0.194071241	0.222910301	0.870624822	0.384007673	−0.242948018	0.6310905
X_2	0.458984586	0.015729695	29.17949689	6.2467E − 171	0.428146264	0.489822908
X_3	0.100335053	0.021574299	4.650675043	3.40788E − 06	0.058038291	0.142631816
X_4	−0.003986937	0.00053663	−7.429576758	1.30705E − 13	−0.005039009	−0.002934864
X_5	−0.358311658	0.015177645	−23.60785562	5.7726E − 116	−0.388067677	−0.328555638
X_6	0.007992118	0.00191096	4.182253507	2.94389E − 05	0.00424565	0.011738585

ijer, 2026, 1, Downloaded from https://onlinelibrary.wiley.com/doi/10.1155/er/1293591 by Hacer AKHAN - Trakya Universitesi , Wiley Online Library on [23/09/2026]. See the Terms and Conditions (https://onlinelibrary.wiley.com/terms-and-conditions) on Wiley Online Library for rules of use; OA articles are governed by the applicable Creative Commons License

TABLE 16 | Regression statistics of the exergy loss coefficient for T_S >45°C.

Regression statistics	
Multiple R	0.952775406
R^2	0.907780974
Adjusted R^2	0.907652206
Standard error (RMSE)	0.824957413
MAE	0.98
Observations	4304

ANOVA test. The multiple R value of 0.95 indicates a very high correlation between the actual values and the predicted values. It shows that the independent variables added to the model truly contribute. In this regression analysis, the obtained F-value (7049.76) is exceptionally high, indicating that the model has strong explanatory power for the dependent variable. Furthermore, the significance $F = 0$ (practically $p < 0.0001$) demonstrates that the model is statistically highly significant overall and that the independent variables collectively exert a meaningful effect on the dependent variable. These results academically confirm that the constructed regression model is both reliable and explanatory in nature. The RMSE value of 0.825 and the MAE value of 0.98 demonstrate the model's predictive performance. Since RMSE is more sensitive to large errors, it highlights the model's deviations, while MAE indicates the average absolute error magnitude. These results show that the model's predictions have a margin of error of approximately 1 unit and that the errors are generally at an acceptable level. However, the significance of error values depends on the data range used; while these levels may be considered high in narrow ranges, they may be viewed as more reasonable in wide ranges. Therefore, the model's accuracy should be evaluated not in isolation from the context but in conjunction with the data scale.

Figure 21 shows the actual and predicted values for energy efficiency multivariate regression. Figure 22 shows the difference

TABLE 17 | ANOVA test results to T_S >45°C.

ANOVA	df	SS	MS	*F*	Significance *F*
Regression	6	28,786.50618	4797.75103	7049.765135	0
Difference	4297	2924.343688	0.680554733	—	—
Total	4303	31,710.84987	—	—	—

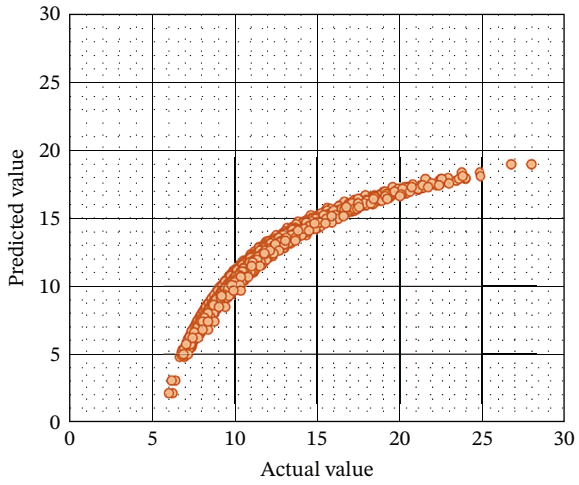


FIGURE 21 | Actual and predicted values for energy efficiency multivariate regression for T_S >45°C.

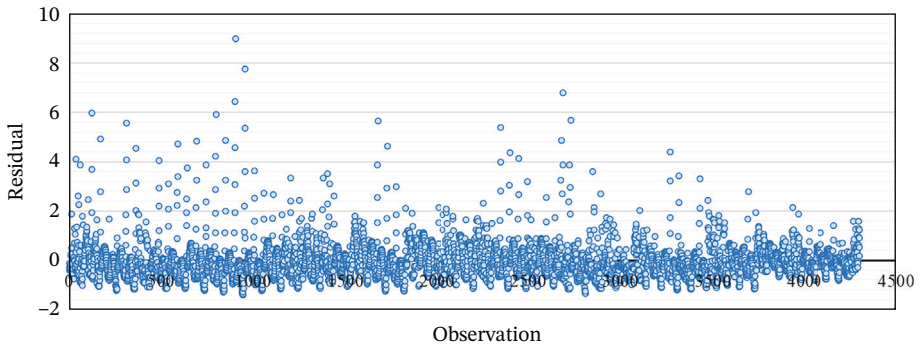


FIGURE 22 | The difference between actual and estimated values for energy efficiency for T_S >45°C.

ijer, 2026, 1, Downloaded from https://onlinelibrary.wiley.com/doi/10.1155/er/1293591 by Hacer AKHAN - Trakya Universitesi , Wiley Online Library on [23/09/2026]. See the Terms and Conditions (https://onlinelibrary.wiley.com/terms-and-conditions) on Wiley Online Library for rules of use; OA articles are governed by the applicable Creative Commons License

between the actual and estimated values for the exergy loss coefficient. While the predictions closely follow the actual values at low levels, the deviation increases at higher values. The fact that the difference between the actual and predicted values is less than 1 indicates that the model operates with high accuracy and that the predictions are reliable. The difference remaining within a range of 1 supports that the model's predictions are practically usable and that its explanatory power for the dependent variable is high.

Regression analysis is one of the most powerful statistical methods used to understand relationships between dependent and independent variables, to predict future values, and to place decision-making processes on a scientific basis. The Equations (25)–(27) obtained as a result of the analysis were derived in order to be able to calculate the dimensionless exergy loss coefficient dependent on PV panel surface temperature in terms of the parameters affecting it, namely, PV panel, type, ambient temperature, wind speed, solar radiation, PV panel surface temperature, and PV panel tilt. Its most important benefit is providing data-driven predictions, enabling the development of more robust and reliable models and ensuring the optimization of energy efficiency and production processes.

4 | Discussion

In this study, energy and exergy analyses of monocrystalline and polycrystalline PV panels were examined for tilts of 0°, 10°, 20°, 30°, and 40° under the climatic conditions of Edirne in August and September 2025. According to the energy analysis results, as the 30° optimum tilt was approached, the highest values of electricity generation were recorded in direct proportion to the solar irradiation. However, at extreme values, such as 0° and 40°, a decrease in energy efficiency was observed due to reflection losses and irradiation losses caused by the cosine effect. Monocrystalline PV panels exhibited a higher conversion efficiency than polycrystalline panels at all tilts, maintaining superior performance even under low solar irradiation.

Evaluations within the framework of exergy analysis provided critical data regarding the thermodynamic sustainability of the system. Although the optimization of the tilt increased the amount of irradiation and thereby increased the electricity production, it also raised the temperature of the panel surface. Exergy efficiency reached its highest values at moderate tilts, where solar irradiation was at its highest and the panel temperature remained close to the ambient temperature. At a 0° tilt, it was determined that the horizontal position of the panel limited cooling through natural convection, leading to increased exergy destruction (irreversibility). At 40°, the ratio of useful work potential (exergy output) to incoming solar exergy decreased due to the reduction in the irradiation input.

In a general comparison, it was found that the exergy efficiency values of monocrystalline panels were approximately 2%–5% higher than those of polycrystalline panels. In PV system installations, determining the optimum tilt appropriate to local geographical conditions to maximize energy production and minimize exergy destruction enhances the thermodynamic performance of the system.

Using the newly defined exergy loss coefficient, the effect of surface temperature on exergy losses has been expressed in a dimensionless form. The exergy loss coefficient measures the relative sensitivity to the temperature increase. The surface temperature-dependent exergy loss coefficient was modeled using multiple regression analysis as a function of panel type, surface temperature, PV panel tilt, solar radiation, ambient temperature, and wind speed.

According to analyses performed with data obtained from experimental studies, the critical temperature at which the tilt of the exergy loss coefficient changes for both panels is in the range of 35°–45°C (310.15–318.15 K). Within the range of critical temperature values, the dimensionless exergy loss coefficient for polycrystalline and monocrystalline silicon PV panels takes values between 19 and 23. For the monocrystalline silicon PV panel, the exergy loss coefficient is lower than that of the polycrystalline PV panel in the range of 1–2. Lower values of the coefficient indicate that the increase in panel surface temperature has a limited effect on exergy loss and that the panel is more resistant to the temperature increase.

The results were obtained by testing monocrystalline silicon and polycrystalline silicon PV panels under the climatic conditions of Edirne during the months of August and September. Any broader generalization of the findings can only be substantiated through the validation of the proposed coefficient across different climatic regions, extended monitoring periods, and alternative PV technologies. Future research is planned to be undertaken on this subject.

Future research should continue to focus on the energy efficiency and exergy analysis of PV panels under different tilts. Predictable climate changes and increasing energy demand make the optimization of renewable energy sources inevitable. In this context, it should be noted that the tilt of PV panels is an effective parameter in the reception of solar radiation and thus in energy production efficiency. In the current literature, studies conducted at specific angles on this topic are generally limited to general observations when evaluating the performance of PV systems in various geographical conditions. Therefore, it would be beneficial for future research to focus on detailing the performance of PV systems in different climate zones and local weather conditions. In addition, exergy analysis should be visualized as a tool for gaining a deeper understanding of the energy conversion processes of PV systems. Existing studies generally focus on energy efficiency, while the examination of exergy losses is not yet sufficiently comprehensive. Future research may contribute to system optimization by developing different models aimed at increasing the exergy efficiency and minimizing losses, especially in integrated PV systems. For example, studies conducted together with additional components, such as cooling systems and solar tracking systems, in addition to panel tilt, have the potential to increase the total energy and exergy efficiency.

Author Contributions

Concept, design, data collection, data analysis/interpretation, writing, critical review: Hacer Akhan. Implementation: Hacer Akhan and Mert Bora Hazar.

ijer, 2026, 1, Downloaded from https://onlinelibrary.wiley.com/doi/10.1155/er/1293591 by Hacer AKHAN - Trakya Universitesi , Wiley Online Library on [23/09/2026]. See the Terms and Conditions (https://onlinelibrary.wiley.com/terms-and-conditions) on Wiley Online Library for rules of use; OA articles are governed by the applicable Creative Commons License

Acknowledgments

This research was financially supported by the Trakya University Scientific Research Project Fund (Project Number TUBAP-2025/123).

Funding

This study was funded by the Trakya Üniversitesi (Grant TUBAP-2025/123).

Conflicts of Interest

The authors declare no conflicts of interest.

Data Availability Statement

The data are available upon request from the authors.

References

1. E. Skoplaki and J. A. Palyvos, "On the Temperature Dependence of Photovoltaic Module Electrical Performance: A Review of Efficiency/Power Correlations," *Solar Energy* 83, no. 5 (2009): 614–624.

2. V.-S. Hudișteanu, N.-C. Cherecheș, F.-E. Țurcanu, I. Hudișteanu, and C. Romila, "Impact of Temperature on the Efficiency of Monocrystalline and Polycrystalline Photovoltaic Panels: A Comprehensive Experimental Analysis for Sustainable Energy Solutions," *Sustainability* 16, no. 23 (2024): 10566.

3. A. Sofijan, M. Khori, W. Adipradana, B. O. Siregar, R. Sipahutar, and S. D. Oktarini, "Evaluation of the Effect of Radiation and Temperature on the Efficiency of Various Types of PV Panels: Monocrystalline, Polycrystalline, and Thin Film," *Semarak Engineering Journal* 9, no. 1 (2025): 38–53.

4. R. Kumar and G. N. Tiwari, "Energy and Exergy Analysis of Photovoltaic Panels With Different Tilt Angles," *Applied Thermal Engineering* 105 (2016): 557–565.

5. A. N. Al-Shamani, "Experimental Investigation of Energy and Exergy Performance of PV Modules Under Different Inclination Angles," *Renewable Energy* 112 (2017): 74–83.

6. M. M. Fouad, L. A. Shihata, and E. I. Morgan, "Comparative Energy and Exergy Analysis of PV Technologies in Mediterranean Climate," *Solar Energy Materials and Solar Cells* 186 (2018): 254–258.

7. H. Xie and M. Lira-Cantu, "Multi-Component Engineering to Enable Long-Term Operational Stability of Perovskite Solar Cells," *Journal of Physics: Energy* 2, no. 2 (2020): 024008.

8. W. Ahmed, J. A. Sheikh, S. Ahmad, S. H. Farjana, and M. A. P. Mahmud, "Impact of PV System Orientation Angle Accuracy on Greenhouse Gases Mitigation," *Case Studies in Thermal Engineering* 23 (2021): 100815.

9. A. Bejan, *Entropy Generation Minimization: The Method of Thermodynamic Optimization of Finite-Size Systems and Finite-Time Processes* (CRC Press, 1996).

10. A. Elbrashy, Y. Boutera, C. Beldjani, M. Abdel-Aziz, K. Balasubramanian, and M. Arıcı, "The Mechatronic Revolution in Renewable Energy: Cross-Domain Synergies With AI and IoT for Efficiency and Resilience," *International Journal of Ambient Energy* 47, no. 1 (2026): 1–20.

11. A. Elbrashy, M. K. El-fakharany, M. A. Al-Sood, F. S. Abou-Taleb, and F. A. Essa, "Development and Performance Evaluation of a Hybrid PV/T Solar Dryer With Steel Mesh Air Channel Enhancement and Independent Forced Air Flow," *Applied Thermal Engineering* 281 (2025): 128650.

12. https://www.harita.tr/edirne (10.08.2026).

13. J. Szargut, *Exergetic Analysis of Thermal Processes* (Institute of Thermal Technology of the Silesian University of Technology, 1996).

14. W. Kuczynski and K. Chliszcz, "Energy and Exergy Analysis of Photovoltaic Panels in Northern Poland," *Renewable and Sustainable Energy Reviews* 174 (2023): 113138.

15. J. Kramarz and A. Wyczesany, *Exergetic Evaluation of Coal Processing Processes Towards Liquid Fuels* (Cracow University of Technology Publishing House, 1991).

16. G. Tsatsaronis, "Definitions and Nomenclature in Exergy Analysis and Exergoeconomics," *Energy* 32, no. 4 (2007): 249–253.

17. K. F. V. Wong, *Thermodynamics for Engineers*, Second ed. (CRC Press, Taylor@Francis Group, 2000).

18. R. Petela, "An Approach to the Exergy Analysis of Photosynthesis," *Solar Energy* 82, no. 4 (2008): 311–328.

19. P. Gilman, A. Dobos, N. DiOrio, J. Freeman, S. Janzou, and D. Ryberg, "SAM Photovoltaic Model Technical Reference Update," National Renewable Energy Laboratory Report NREL/TP-6A20-67399 (2018).

20. P. Ravat, "Exergy Performance Analysis of 300 W Solar Photovoltaic Module," *International Journal of Engineering Sciencesve Research Technology* 3 (2017): 317–390.

21. C. E. B. Elhadj Sidi, M. L. Ndiaye, A. Ndiaye, and P. A. Ndiaye, "Outdoor Performance Analysis of a Mono Crystalline Photovoltaic Module: Irradiance and Temperature Effect on Exergetic Efficiency," *International Journal of Physical Sciences* 10, no. 11 (2015): 351–358.

22. K. Sudhakar and T. Srivastava, "Energy and Exergy Analysis of 36 W Solar Photovoltaic Module," *International Journal of Ambient Energy* 35, no. 1 (2014): 51–57.

ijer, 2026, 1, Downloaded from https://onlinelibrary.wiley.com/doi/10.1155/er/1293591 by Hacer AKHAN - Trakya Universitesi , Wiley Online Library on [23/09/2026]. See the Terms and Conditions (https://onlinelibrary.wiley.com/terms-and-conditions) on Wiley Online Library for rules of use; OA articles are governed by the applicable Creative Commons License